https://doi.org/10.5194/hess-2021-377
Preprint. Discussion started: 22 September 2021

Hydrology and Earth System Sciences Discussions

The Spatiotemporal Regime of Glacier Runoff in Oases Indicates the Potential Climatic Risk in Dryland Areas of China

Xuejing Leng[1,2], Xiaoming Feng[1], Bojie Fu[1], Yu Zhang[1,2]

[1]State Key Laboratory of Urban and Regional Ecology, Research Centre for Eco-Environmental Sciences, Chinese Academy of Sciences, Beijing, 100085, China

[2]University of Chinese Academy of Sciences, Beijing, 100049, China

Correspondence to: Xuejing Leng (xjleng_st@rcees.ac.cn)

Abstract. Glaciers continuously affected by climate change are of great concern; their supply and runoff variation tendency under the pressure of increasing populations, especially in dryland areas, should be studied. Due to the difficulty of observing glacier runoff, little attention has been given to establishing high-resolution and long-term series datasets established for glacial runoff. Using the latest dataset using digital elevation models (DEMs) to obtain regional individual glacier mass balance, simulating the spatiotemporal regime of glacier runoff in oases that support almost the entire income in the dryland areas of China (DAC) could be possible. The simulations quantitatively assess glacier runoff, including meltwater runoff and delayed runoff, in each basin of the DAC at a spatial resolution of 100 m from 1961 to 2015, classify glaciers according to the potential climatic risks based on the prediction results. The total glacier runoff in the DAC is $(98.52 \pm 67.37) \times 10^8$ m^3, in which the meltwater runoff is $(63.43 \pm 42.17) \times 10^8$ m^3, accounting for 64.38%. Most basins had continuously increasing tendencies of different magnitudes from 1961 to 2015, except for the Shiyang River basin, which reached its peak in approximately 2000. Glacier runoff nurtured nearly 143,939.24 km^2 of oasis agricultural areas (OAA) until 2015, while 19 regions with a total population of 14 million were built alongside the oases, where glacier runoff occupies an important place in agricultural, industrial and municipal water consumption. Therefore, providing a long time series of glacier runoff for different river basins is of great significance to the sustainable development of the oasis economy in the arid zones.

Key words. Glacier runoff, Oases, Dryland areas of China, Spatiotemporal regime

1 Introduction

Persistently affected by climate change, the cryosphere has a tremendous impact on global hydrology and water resources (Adler et al., 2019; Beniston & Stoffel, 2014; Bibi et al., 2018; Ding et al., 2006; Piao et al., 2010; Sorg et al., 2012). Research on snow and ice is in line with the corresponding targets of the Sustainable Development Goals (SDGs) (Avtar et al., 2019; Bolch et al., 2019; Gratzer & Keeton, 2017; Hinz et al., 2020; Rasul et al., 2019; Wu et al., 2018) and 2 goals in the Intergovernmental Science-Policy Platform on Biodiversity and Ecosystem Services (IPBES) (Arora & Mishra, 2019; Compagno et al., 2021; Hausner et al., 2020; Keller et al., 2019; Martin-Lopez et al., 2019). Glaciers are the largest reservoirs of fresh water on Earth, and they store most of the ice and snow (Beniston & Stoffel, 2014; Kraaijenbrink et al., 2017). Glaciers store water as ice in the colder months and release it as meltwater as warmer summer temperatures melt the glaciers, creating runoff that carries valuable fresh water downstream for the benefit of human society (Immerzeel et al., 2012; Laghari et al., 2012; Qin et al., 2006; Yang et al., 2019), mitigating drought (Kaser et al., 2010; Wang et al., 2021) and poverty (Wang, Zhou, et al., 2020; Zarfl et al., 2015). Under current climate conditions, warming causes glaciers to melt and sea levels to rise, creating a negative feedback between the two (Brun et al., 2017; Shean et al., 2020).

An oasis is a special combined landscape of nature and humanity, and oases are essential in arid areas (Shi et al., 2003; Zhu et al., 2019). Oases in the dryland areas of China (hereafter DAC) support 90 percent of local residents and generate more than 95 percent of social wealth (Bie & Xie, 2020) in areas where agriculture relies on river channels (Biemans et al., 2019; Immerzeel et al., 2012). Most river basins in the DAC depend most on glacier runoff, which is a high-altitude water resource (Chen et al., 2016; Huang et al., 2009; Li et al., 2011; Zhang, Liu, et al., 2016), and glacier runoff is sometimes the only source of water for some oasis agriculture areas (OAAs) (Waldron et al., 2020), especially in the Hexi Corridor (Li et al., 2018). Under the high demand for water as a result of the rapidly growing population and irrigation combined with the arid climate in the DAC (Barnett et al., 2005; Fan et al., 2013; Immerzeel & Bierkens, 2012), the importance of water provided by glaciers in arid regions is apparent (Barnett et al., 2005; Pritchard, 2019; Tak & Keshari, 2020; Wang et al., 2021). Affected by global

https://doi.org/10.5194/hess-2021-377
Preprint. Discussion started: 22 September 2021

warming, the rapid change in the cryosphere and its interactions with the biosphere, lithosphere, hydrosphere, atmosphere, and anthroposphere are increasingly intensified, having especially extensive and profound impacts on hydrology, water resources, ecosystems (Sun et al., 2020; Zhang, Liu, et al., 2019), and the sustainable development of the human economy and society (Lin et al., 2020).

Field observation is by far the most accurate method used to obtain individual glacier mass balance and was used to establish the first and second glacier catalogs in China in the 1970s and the early 21st century, respectively (Liu et al., 2015; Sun et al., 2018). Continuous yearly mass balance data for long time series could not be calculated effectively due to the time consumption and high energy consumption of field observations (Brun et al., 2017; Shean et al., 2020). Therefore, the energy balance equation was used to reconstruct the glacier mass balance (Sakai et al., 2015; Yao et al., 2010) based on remote sensing datasets (Hussain et al., 2019) or imagery (Tak & Keshari, 2020), and the snow line was identified to be approximately the same as the equilibrium-line altitude (ELA). Another method used to calculate glacier runoff focuses on establishing the relationship between runoff and air temperature through meteorological station data with the degree-day factor model to better reflect the role of temperature in meltwater (Li et al., 2020; Liu, Zhang, et al., 2019). Semi-distributed hydrological models were also used to estimate the contribution of meltwater runoff to river flow, and similarly, river isotopic studies (Duan et al., 2020; Garee et al., 2017; Zhang, Luo, et al., 2016). However, some limitations were obvious: the relationship between stations and the degree-day factor model was too difficult to establish in large regions, while the energy balance model could be applied in large regions but with low resolution (such as 0.25 degrees (Sakai et al., 2015)). Semi-distributed hydrological models semi-quantitatively calculated the proportion of meltwater runoff to total runoff without time series. Taking advantage of digital elevation models (DEMs), some studies (Brun et al., 2017; Shean et al., 2020) have published mass balance datasets with high resolution; the former were 30 m based on the single-source Glacier Area Mapping for Discharge from the Asian Mountains (GAMDAM) inventory (Sakai, 2018), and the latter were accurate to each individual glacier based on the multisource Randolph Inventory (RGI Consortium, 2017), which makes estimating high-resolution glacier runoff data possible.

We used the mass balance equation and dataset with high resolution to inversely reconcile high-altitude precipitation and then estimate the yearly ablation and accumulation to obtain glacier runoff time series. The first aim of this study was to totally quantify glacier runoff rather than qualify (Yang et al., 2015; Ye et al., 2017) or semi-quantify (Kayastha et al., 2020; Kumar et al., 2019; Mimeau et al., 2019; Wang et al., 2015) runoff in watersheds of the DAC. Second, the two parts of glacier runoff, which are called delayed runoff and meltwater runoff, were identified quantitatively and their impacts on the OAAs in the DAC were assessed. Additionally, the overall trend of glacier runoff was discerned, including the change trend and turning point of the two components. The spatial resolution of this study was improved to 100 m from 0.25 and 0.5 degrees in previous studies, and glacier runoff time series were observed with a time span of 54 years. By improving the spatial resolution, extending the temporal scope and correcting high-mountain precipitation and temperature, this paper provides a more accurate dataset for the evaluation of cryospheric ecological security patterns and ecosystem services in the future as well as a more scientific basis for sustainable cryospheric development.

2 Materials and methods

2.1 Observations

This paper used daily precipitation datasets from the Asian Precipitation – Highly Resolved Observational Data Integration Towards Evaluation Of Water Resources MA_v1101 and MA_v1101_EXR1 (APHRODITE) at a 0.25° spatial resolution for the period 1961-2015 in monsoon Asia (http://aphrodite.st.hirosaki-u.ac.jp/product). The gridded daily temperature data were taken from the APHRODITE MA_1808_TEMP (http://aphrodite.st.hirosaki-u.ac.jp/product) dataset at a spatial resolution of 0.25° for the period 1961-2015. Information about glacier outlines, elevations and areas was derived from the Randolph Glacier Inventory (version 6.0, https://www.glims.org/RGI/rgi60_dl.html). We used the SRTM DEM with a resolution of ~100 m (version 4.1, http://srtm.csi.cgiar.org). We obtained river basin outlines as shape files from the Resource and Environment Science and Data Center of the Institute of Geographic Sciences and Natural Resources Research, Chinese Academy of Sciences (http://www.resdc.cn/data.aspx?DATAID=278). The glacier mass balance data were derived from Shean' estimations (Shean et al., 2020) (https://zenodo.org/record/3600624). The dataset of the spatial distribution of degree-day factors for

https://doi.org/10.5194/hess-2021-377
Preprint. Discussion started: 22 September 2021

glaciers was obtained from the Science Data Bank (http://www.sciencedb.cn/dataSet/handle/747) at a spatial resolution of 0.5° in High Mountain Asia and contained snow-melt and ice-melt degree-day factor distributions. Oases information was obtained from Copernicus Global Land Service (CGLS) LC100 collection 3 at a spatial resolution of 100 m on Google Earth Engine (GEE) (http:/land.copernicus.eu/global/products/lc).

2.2 Study Area

By using the ratio data of annual precipitation to annual evapotranspiration (aridity index, AI), the DAC was obtained relying on drought zoning supported by the United Environment Programme (UNEP), which erased the range of the Tibetan Plateau, which is discussed separately. There are seven glacier regions around the DAC, including the Qilian Shan, Eastern Kunlun, Western Kunlun, Eastern Tien Shan, Western Tien Shan, Karakoram, and Pamir, which include approximately 42,000 glaciers involving four provinces: Inner Mongolia, Xinjiang, Gansu and Qinghai. The 7 glaciers affect 22 tertiary watersheds in the DAC, including 6 drainage basins which all originated directly from glaciers and across arid and hyper-arid regions (hereafter, AH). 2 river basins were both completely in the arid zone while 11 drainage basins were in both semiarid and arid regions (hereafter, SA). The Datong River above the Hall basin was the single basin entirely in the semiarid zone, and the Qarqan Rivers Basin was across semiarid, arid and hyper-arid zones (hereafter SAH). As Table 1 shows, the area of OAAs in each watershed in the DAC reached a maximum of 21,699.18 km^2 (Middle Rivers basin), with an average of 6543.692 km^2, while the precipitation in the DAC reached a maximum of 323.09 mm (Qinghai Lake Drainage System), with an average of 134.56 mm, which revealed that runoff in the DAC was extremely important, especially in some basins where runoff originated almost entirely from glaciers. The study area is shown in Fig. 1.

https://doi.org/10.5194/hess-2021-377
Preprint. Discussion started: 22 September 2021

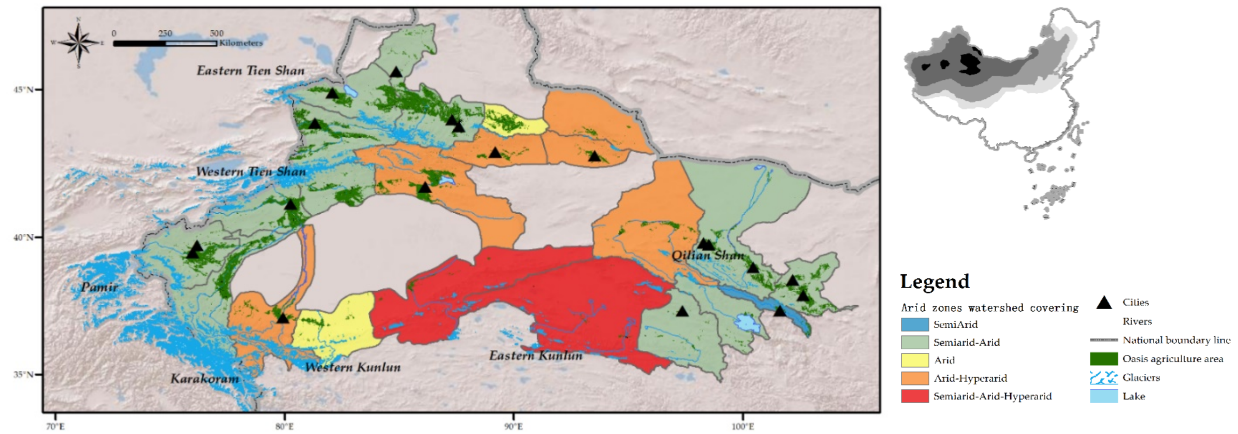

Fig. 1. Locations of watersheds and oasis agriculture areas affected by glaciers in the dryland areas of China. (Shades of colour indicate drought from subhumid – semiarid – arid – hyper-arid) and the tertiary watersheds in the dryland areas of China affected by the Qilian Shan, Western Tien Shan, Eastern Tien Shan, Western Kunlun, Eastern Kunlun, Karakoram and Pamir. Oasis agricultural areas exist along rivers that originate from glaciers, and cities are built around oases. World Shaded Relief provided by Esri (http://goto.arcgisonline.com/maps/World_Shaded_Relief) and the Chinese map was from Resource and Environment Science and Data Centre, Chinese Academy of Sciences (https://www.resdc.cn/data.aspx?DATAID=205).

Table 1. Annual precipitation and area of OAA in each watershed.

Watershed	Annual precipitation (mm)	Area of OAA (km^2)
Pai Basin	93.06	1047.50
Shule River Basin	79.10	2913.70
Hami Basin	63.53	1585.64
Turpan Basin	75.94	2218.58
Kai-kong River Basin	103.92	10191.39
Hotan River Basin	39.04	4816.73
Western Qaidam Basin	~ 0	538.37

Eastern Qaidam Basin	~ 0	876.23
Kriya Rivers Basin	51.31	2308.90
Qarqan Rivers Basin	78.82	1362.69
Easter Rivers Basin	139.52	5487.35
Middle Rivers Basin	175.29	21699.18
Yarkand River Basin	99.87	13568.21
Kashgar River Basin	137.61	11027.69
Weigan River Basin	136.96	8632.32
Aksu River Basin	148.64	10276.95
Qinghai Lake Drainage System	323.09	1012.96
Ebinur Lake Drainage System	191.29	11366.95
Heihe River Basin	113.67	9273.28
Shiyang River Basin	198.63	9333.13
Ili River Basin	299.05	13332.06
Datong River Above Hall	410.38	1069.43

2.3 Methods

2.3.1 Reconciling High-altitude Precipitation

We used geodetic mass balance estimates in the high-mountain Asia (HMA) between 2000 and 2018 by combining reprocessing ASTER DEMs (hereafter Shean estimation (Shean et al., 2020)) to simulate high-altitude precipitation. The mass balance, B_y(m), is the sum of accumulation, A_C(m), and ablation, A_b(m), at a yearly time step following Eq. (1):

$$B_y = A_b + A_c = \int_{t_1}^{t} (A_b + A_c)dt, \quad (1)$$

Hydrology and Earth System Sciences
Open Access
EGU
Discussions

The yearly mass balance was obtained from the Shean estimation. A comparison of Shean estimation to mass balance estimates was improved by Brun et al. (Brun et al., 2017) between 2000 and 2016 using ASTER DEMs (here after Brun estimation) and trends based on NASA's Ice, Cloud and Land Elevation Satellite (ICESat-1) data for the period 2003-2008 (here after ICESat data) (Immerzeel et al., 2015; Kaab et al., 2012; Srivastava et al., 2013), and the total HMA glacier mass loss was -0.19 ± 0.03 m w.e. a^{-1} from 2000 to 2018 (Shean estimation), -0.18 ± 0.04 m w.e. a^{-1} from 2000 to 2016 (Brun estimation) and -0.40 ± 0.09 m w.e. a^{-1} from 2003 to 2008 except in the region of Eastern Kunlun, Qilian Shan and Inner Tibet (ICESat data). While the ICESat data did not reflect small glaciers, the data were used to calculate the elevation changes of glaciers larger than 5 km^2 in area and then to interpolate the elevation variations across the entire region, and the satellite no longer provided data in 2009. In view of the applicability of time range and spatial resolution, ICESat data were not described in this paper. Because the algorithms of the Brun estimation and Shean estimation were analogous, this paper focused on comparing the Shean estimation and Brun estimation to handle a more appropriate dataset. Based on the RGI 6.0, 6 glacier regions influence the DAC. Mass changes in the Eastern Kunlun and Karakoram were -0.01 ± 0.07 m w.e. a^{-1} (Brun estimation) and -0.02 ± 0.15 m w.e. a^{-1} (Shean estimation), -0.03 ± 0.07 m w.e. a^{-1} (Brun estimation) and -0.05 ± 0.13 m w.e. a^{-1} (Shean estimation), where the Karakoram anomaly was consistent with the former studies. Both of the positive mass change estimations were in Western Kunlun (Brun estimation was 0.16 ± 0.08 m w.e. a^{-1} and Shean estimation was 0.10 ± 0.17 m w.e. a^{-1}). Both of the negative mass change estimations were in Western and Eastern Tien Shan (Brun estimation was -0.20 ± 0.08 m w.e. a^{-1} and -0.40 ± 0.20 m w.e. a^{-1} while Shean estimation was -0.22 ± 0.33 m w.e. a^{-1} and -0.42 ± 0.25 m w.e. a^{-1}). Mass changes in the Qilian Shan were -0.29 ± 0.08 m w.e. a^{-1} (Brun estimation) and -0.29 ± 0.25 m w.e. a^{-1} (Shean estimation). The two estimates for each region of the DAC were generally similar (-0.95 m w.e. a^{-1} (Shean estimation) vs. -0.83 m w.e. a^{-1} (Brun estimation)) with large differences between uncertainty (1.37 m w.e. a^{-1} (Shean estimation) vs. 0.65 m w.e. a^{-1} (Brun estimation)). This paper selected the Shean estimation to simulate mass balance for recording mass balance and uncertainty of each individual glacier, multisource RGI v6.0 glacier inventory (while the Brun estimation used the single-source GAMDAM inventory) and implemented robust approaches to estimate elevation change trends for each glacier.

The degree-day factor (DDF) is an important parameter reflecting the amount of ice and snow melt generated by the unit positive accumulated temperature (Kaser et al., 2010; Kraaijenbrink et al., 2017). Previous studies have generally used 2 mm °C^{-1} d^{-1} as the DDF for snow melt (Azam et al., 2012; Immerzeel et al., 2015). The spatial variation in the DDF has a great influence on the accuracy of simulating the snow melt process. This paper used the spatial distribution of snow melt data with a resolution of 0.5° based on a formula built by investigations and observations of 40 different glaciers in the HMA, and the dataset verified the accuracy (Zhang et al., 2006). Considering that the spatial resolution of this paper was 100 m, monthly positive-degree days (PDD_m) were chosen instead of absolute PDD (Braithwaite & Olesen, 1993), and they were the summed positive daily average temperatures. The monthly spatial distribution of ablation, $A_{b,m}$(m), was calculated by the product of DDF and PDD_m when the sum of the twelve months was the yearly spatial distribution of ablation, $A_{b,y}$(m). The accumulation at a daily step depends on temperature, while precipitation is separated into solid (snow, A_c(m)) and liquid (rain) by temperature. The relationship between snowfall and temperature was as follows: the temperature at which all precipitation becomes liquid was assumed to be 4°C, T_1(°C), the actual temperature, T_a(°C) and the daily corrected precipitation, $P_{cor,d}$(m) (Fujita & Nuimura, 2011; Sakai et al., 2015) following Eq. (2):

$$A_c = \begin{cases} P_{cor,d}, T_a \leq 0 \\ \left(1 - \frac{T_a}{T_1}\right) P_{cor,d}, 0 < T_a \leq T_1, \\ 0, T_a > T_1 \end{cases} \quad (2)$$

The maximum rainfall height and maximum elevation of glaciers around the DAC were obtained from RGI v6.0 and used as the basis for high-altitude precipitation estimation by calculating the vertical precipitation gradient (Immerzeel et al., 2015). We used the Shean estimation to optimize the precipitation gradient per glacier. At each glacier affecting the DAC, the corrected precipitation, $P_{cor,d}$ (m), was calculated as a function of original precipitation data from APHRODITE_MA_v1101_EXR1, $P_{rmd,d}$(m), the vertical precipitation gradient, PG(% m^{-1}), at a daily time step with the maximum precipitation altitude, H_{map}(m), maximum elevation, H_{max}(m), and terrain elevation, H(m), for each individual glacier, using the following Eq. (3) and Eq. (4):

$$\Delta H = H_{max} - H_{map}, \quad (3)$$

$$P_{cor,d} = P_{rmd,d} \cdot \{1 + [\Delta H + (H_{max} - H)] \cdot PG \cdot 0.01\}, \quad (4)$$

Each glacier from seven regions of glaciers around the arid area of China was simulated, and then the vertical precipitation gradients that were generated were interpolated to obtain a wide range of vertical precipitation gradients representing the change in precipitation with altitude. By using the nearest neighbor algorithm for aggregating (López-Granados et al., 2005), the vertical precipitation gradient at a spatial resolution of 0.25° was obtained.

2.3.2 Glacier Runoff

Glacier runoff is defined as the flow of meltwater from a glacier through ice, in and under ice and then into a river channel (Qin et al., 2021). Based on the definition of glacier runoff, the runoff includes two parts. One is the precipitation on glaciers stored in the non-melting season and released in the melting season, which is called delayed runoff (Kaser et al., 2010; Pritchard, 2019; Shean et al., 2020). The monthly delayed runoff during the ablation seasons, ΔM_m(m), was calculated by the difference in the proportion of total annual corrected precipitation, $P_{cor,y}$(m), allocated to the ablation season runoff, $M_m(m)$, according to the proportion of monthly PDD, PDD_m and yearly PDD, PDD_y. The ablation season was defined as all months in which the monthly temperature was above T_a. M_m was calculated as the following Eq. (5):

$$M_m = P_{cor,y} \times PDD_m / PDD_y, \tag{5}$$

When the temperature was above T_a, freezing did not occur on the surfaces of the glaciers, and precipitation occurred as liquid rainfall on the glacier that flowed out of the glacier systems in the form of runoff. If the runoff allocated in the month, $M_m(m)$, was more than the corrected precipitation in the month, $P_{cor,m}(m)$, delayed runoff, ΔM_m(m), occurred while the glaciers stored the solid precipitation in the accumulation seasons and released it in the ablation seasons following Eq. (6):

$$\Delta M_m = M_m - P_{cor,m}, \tag{6}$$

The delayed runoff calculation method was proposed by Kaser et al. (Kaser et al., 2010) and improved by Pritchard (Pritchard, 2019) for regional calculations. This method, where the precipitation dataset is the most important component, provides the possibility of calculating the monthly delayed runoff for a long time series and on a regional scale.

Based on the verification precipitation data (V2.0) (http://data.cma.cn/) provided by the China Meteorological Data Service Centre (CMDSC) from 1998 to 2016, Zhang (2020) generated a scatter plot and found that APHRODITE had the highest determination coefficient (compared with TRMM, Tropical Rainfall Measuring Mission (https://gpm.nasa.gov/missions/trmm), and ITPCAS (China meteorological forcing dataset, (Jie & Kun, 2016)) and had the best applicability in Tien Shan of China. Han and Zhou (2012) found that the correlation coefficient between APHRODITE and ground gauge observed precipitation was more than 0.9, and APHRODITE explained spatial heterogeneity better (Yatagai et al., 2014) because it considered topography in the process of spatial interpolation (Yang et al., 2014). Li et al. showed that APHRODITE reflected the spatial and temporal distribution characteristics of precipitation in inland river basins and then compensated for the shortage of spatial precipitation data in the study area (Li et al., 2014). Tan et al. evaluated APHRODITE, CHIRPS (Climate Hazards Group InfraRed Precipitation with Station, https://data.chc.ucsb.edu/products/CHIRPS-2.0/), and PERSIANN-CDR (Precipitation Estimation from Remote Sensing Information using an Artificial Neural Network – Climate Data Record, https://climatedataguide.ucar.edu/climate-data/persiann-cdr-precipitation-estimation-remotely sensed-information-using-artificial) on the Tibetan Plateau and its surrounding areas and found that APHRODITE performed best with the longest time span (> 50 years) and had a higher R^2 with a lower MAE and RMSE than that of CHIRPS and PERSIANN-CDR (Tan et al., 2020). APHRODITE had the best performance in the DAC, including the Heihe River basin (Tang et al., 2017), Qinghai Lake drainage system (Zhang et al., 2014), Xinjiang (Wang, Sun, et al., 2020), upper reaches of the Yellow River (Guan et al., 2020) and other mountainous areas (Mishra et al., 2019). Therefore, we used APHRODITE, which has been verified many times and is one of the most accurate precipitation records in the DAC, in this paper.

The precipitation was corrected by the Shean estimation for high-altitude precipitation gradients in this paper for the glaciers affecting the DAC. Reconciling high-altitude precipitation and then recycling the former method to calculate the delayed runoff at a one-month time step for each glacier basin would be more persuasive without relying on the original products (Wortmann et al., 2018). Sakai et al. (Sakai et al., 2015) corrected the on-glacier precipitation by assuming that the average mass balance from 1979 to 2007 was equal to 0 at the ELA, referring to the median elevations of glaciers larger than 1 km^2 and the area-weighted average in each 0.5 grid using the glacier inventory (GGI) in High Mountain Asia on the basis of APHRODITE. The ELA is called the L-elevation, and the on-glacier precipitation was adjusted by one ratio at a resolution of 0.5°, while the ratios in the seven glacier regions affecting the DAC were 1-3 (Qilian Shan), 0-7 (Eastern Tien Shan), 0-4 (Western Tien Shan), 3-

https://doi.org/10.5194/hess-2021-377
Preprint. Discussion started: 22 September 2021

Hydrology and Earth System Sciences
Open Access
Discussions

7 (Western Kunlun), 0-4 (Eastern Kunlun) and 0-10 (Karakoram, with an extremely large ratio grid). The precipitation gradient factor with altitude was calculated based on the mass balance of each single glacier at a more accurate spatial resolution of 100 m in this paper.

The second type of glacier runoff was runoff from melting glaciers called excess meltwater runoff. Pritchard (Pritchard, 2019) calculated the excess flow of meltwater provided to the HMA river basins through a regional geodetic study of glacier volume changes from 2000 to 2016 by Brun (Brun et al., 2017), namely, the Brun estimation. Unlike delayed runoff due to precipitation, excess meltwater runoff is based on measured mass balance changes in glaciers rather than on average climate, so this runoff component is also called an unbalanced component, while the runoff caused by precipitation is called a balanced component (Rounce, Hock, et al., 2020; Rounce, Khurana, et al., 2020). With the Brun estimation, due to the time limit from 2000 to 2016, the contribution of unbalanced components to water input at the start of the 21st century compared with the balance components such as long-term precipitation could be obtained. Brun estimated that the excess water in the catchments controlled by the HMA, including the Yangtze, Mekong, Salween, Brahmaputra, Ganges, Indus, Amu Darya, Tarim, Syr Darya, Ili, and Inner Tibetan Plateau, was (-14.7 ± 3.2) $km^3\ a^{-1}$ equivalent during 2000-2016 (Brun et al., 2017), which was approximately 70% of the balance component calculated above. The regional basin-scale imbalance uncertainty ranged from 26% to 77%. The Shean estimation estimated that the total excess water flow for all of the river basins originating from 2000 to 2018 was (-22.71 ± 3.01) Gt per year (Shean et al., 2020), where the additional basins considered included the Yellow River, Inner Tibetan Plateau Extended and Irrawaddy. The basin-scale imbalance uncertainty ranged from 12% to 52%. In conclusion, the yearly total glacier runoff, R_y(m), was calculated by the following Eq. (7):

$$R_y = M_y + B_y, \tag{7}$$

Both the Shean estimation and the Brun estimation calculated the average glacier meltwater over the corresponding periods of 2000 to 2018 and 2000 to 2016, respectively. We used the Shean estimation to calculate the precipitation gradient, and then the series of mass balances could be calculated according to Equation 1. Relying on the simulations of ablation and accumulation in reconciling high-altitude precipitation, the time series data of 1961-2015 could be obtained by using the APHRODITE temperature and precipitation data. This paper obtained the time series of meltwater from 1961 to 2015, rather than the mean meltwater in a certain period of time (Pritchard, 2019; Shean et al., 2020). Time series data have unique advantages for studying the change trend and can also more clearly observe the change in meltwater within any required time period.

We provide a method to predict future total glacier runoff relying on temperature, precipitation and elevation data, as both of the goals of the Representative Concentration Pathway (RCP) and the Coupled Model Intercomparison Project (CMIP) are keeping the increase in temperature within a certain range. PG in this paper was obtained by interpolation using the mass balance algorithm and geostatistics method. Glacier runoff was divided into delayed runoff and excess meltwater runoff.

2.3.3 Uncertainty Analysis

According to the individual glacier uncertainty (including random error and systematic error) calculated in the Shean estimation, the uncertainty range of glacier mass balance changes could be obtained. The maximum and minimum values of a single mass balance were calculated through the uncertainty interval. Referring to the H_{max} provided by the RGI and H_{map} referred to previous studies and reasonable inference of H_{min} in the RGI, the PG of each single glacier around the DAC was obtained by geographical simulation. After using the DDF model and the glacier mass balance model, the corrected precipitation and meltwater were obtained, which were the bases of delayed runoff and meltwater runoff, respectively. The uncertainty of glacier runoff was the precipitation gradient in the range obtained from the uncertainty of glacier mass balance and was then calculated according to the relevant models. Calculations of delayed runoff and meltwater runoff and their uncertainties were shown in the Fig. 2 where shaded blocks were results with uncertainties. The uncertainties of delayed runoff and meltwater runoff value in this paper came from the uncertainties of mass balance in Shean estimation because obtaining from remote sensing observation accompanied by a large uncertainty value.

Hydrology and Earth System Sciences
Discussions

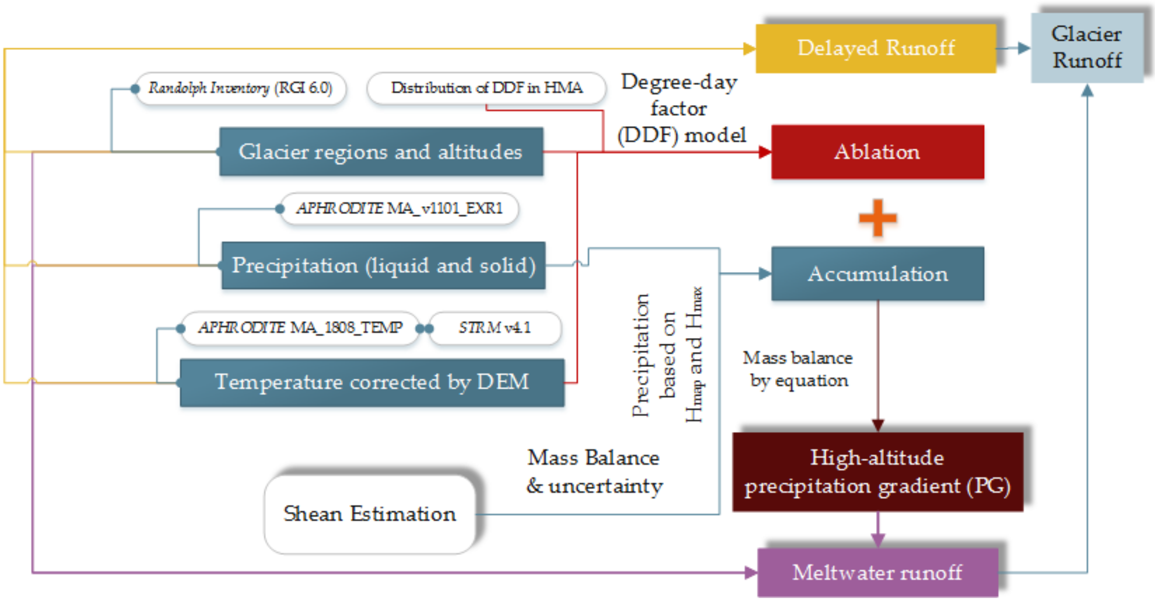

Fig. 2. Conceptual framework of glacier runoff calculating. Blocks represent module of the glacier runoff calculation in each category. Shading indicated results with uncertainties and different lines and blocks indicated the corresponding modules.

2.3.4 Trend Analysis

The Mann-Kendall test (MK test) was recommended as an effective method to distinguish whether a natural process is in a natural fluctuation or has a definite trend of change especially for hydro-meteorological data with non-normal distribution (Mann, 1945; Kendall, 1975). Given a time series $x(t)$ of length n with statistical hypothesis that the unadjusted data series was an independent random variable with the same distribution composed of n elements. m_i represented the cumulative number of $x(i)$ was greater than $x(j), 1 \leq j \leq i$, and the statistic d_k was defined as following Eq. (8):

$$d_k = \sum_{i=1}^{k} m_i \, , 2 \leq k \leq n, \tag{8}$$

The mean $E(d_k)$ and variance $var(d_k)$ was calculated by the following Eq. (9) and Eq. (10):

$$E(d_k) = k(k-1)/4, \tag{9}$$

$$\mathrm{var}(d_k) = k(k-1)(2k+5)/72, \tag{10}$$

After standardizing d_k, UF_k and UB_k can be calculated as following Eq. (11) and Eq. (12):

$$UF_k = \frac{d_k - E(d_k)}{\sqrt{var(d_k)}}, \tag{11}$$

https://doi.org/10.5194/hess-2021-377
Preprint. Discussion started: 22 September 2021

Hydrology and Earth System Sciences Discussions
Open Access EGU

$$\begin{cases} UB_k = -UF_k \\ k = n + 1 - k, k = 1,2,3,\cdots,n' \end{cases} \tag{12}$$

UF_k formed a UF curve and UB_k formed a UB curve, while the intersection point of the former two curves in the confidence interval was determined as the turning point. While $UF > 0$, it indicated an increasing trend of the sequence, on the contrary, it indicated a declining trend while $UF < 0$.

3 Results

3.1 Glacier Runoff during 1961-2015

In this paper, we used the Shean estimation to correct the high-altitude precipitation gradient and the DDF model to calculate the total glacier runoff around the DAC during 1961-2015 with a spatial resolution of 100 m, and we overcame the difficulty of large-scale geodetic mass balance assessment. Glacier runoff included delayed runoff that was stored rainfall in the cold seasons and released rainfall in the ablation seasons, while meltwater runoff was caused by glacier mass balance, which was also called excessive meltwater runoff or the imbalanced part of glacial runoff, as shown in Fig. 3. The average glacier runoff in the DAC for the period was $(98.52 \pm 67.37) \times 10^8$ m^3, where the meltwater runoff accounted for 64.71%. The drainage basins affected by the glaciers surrounding the DAC were largely controlled by meltwater runoff. The total glacier runoff in the Datong River above the Hall basin, Shiyang River basin, Heihe River basin and Eastern Rivers basin came from excessive meltwater. A total of 78.85% and 61.98% of the glacial runoff in the Aksu River basin and Kashgar River basin originated from glacier mass loss from Western Tien Shan and Pamir, respectively. The delayed runoff components of the Hotan River basin and Yarkand River basin, which originated from Western Kunlun, Karakoram and Pamir, were both larger than the mass balance component. The delayed runoff component of the Qarqan Rivers basin, which was controlled by Western Kunlun and Qilian Shan, reached 73.19%. The creeks of the Kriya Rivers basin were the most unique, with 93.67% of the components coming from delayed runoff; therefore, more attention should be paid to glacier disasters in this basin. Meltwater runoff accounted for 90% or more of the runoff in the remaining basins.

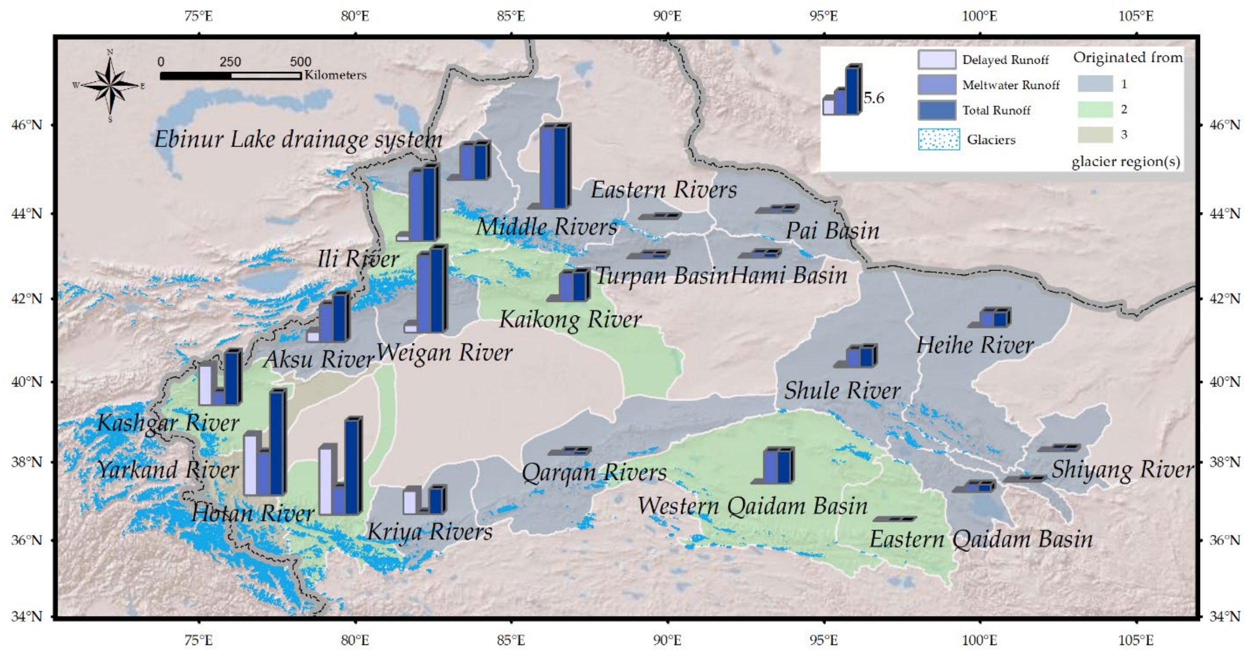

Fig. 3. Map of total glacier runoff. Distribution of total glacier runoff, including delayed runoff and meltwater runoff. Shown are the average amount of runoff for every study basin in the DAC for the period 1961-2015. World Shaded Relief provided by Esri (http://goto.arcgisonline.com/maps/World_Shaded_Relief).

Total glacier runoff had an increasing trend after the 1970s that was significant after the 1990s, with a confidence of 95% in the whole study area. Except for the Datong River above Hall, Heihe River basin and Shiyang River basin, the runoff of the other basins showed continuous increasing trends in the past 50 years, where the times of arrival of significant increase were different. Trends in the Ebinur Lake Drainage System and Kai-kong River basin were significant after the 2000s, the Hotan River basin and Kashgar River basin were significant after the 1980s, and the Qinghai Lake Drainage System, Shule River basin and Aksu River basin showed gradual increasing trends with no significance until 2015. The amount of glacier runoff in the Datong River above Hall began to decrease after the 1990s, and in the Heihe River basin, it decreased after 1995 with no significance according to the Mann-Kendall (MK) test. Glacier runoff in the Shiyang River basin began to decline in 2000 and even showed a significant declining trend in approximately 2010, which was consistent with previous studies (Zhang et al., 2015). The time series of delayed runoff and meltwater runoff for all basins were illustrated in Extended Data Fig. 1, 2 and 3.

Hydrology and Earth System Sciences Discussions

Glaciers stored, on average, $(35.09 \pm 25.20) \times 10^8$ m^3 of water during the period from 1961 to 2015 and released this water during the ablation seasons. The flood lakes and natural hazards caused by this effect require attention. Due to the differences in regional climate and topography, the temperatures and ablation seasons were also different. The total delayed runoff in the study area increased continuously from 1970, and then it reached a turning point and became significant after 1991.

In many basins, such as the Heihe River basin, Turpan Basin, Shiyang River basin, Eastern Rivers basin, and Datong River above Hall basin, the glacier runoff in the DAC was almost all excessive meltwater runoff. From 1961 to 2015, Glaciers in the arid regions provided (63.43 ± 42.17) × 108 m3 of glacial excess meltwater. While focusing on current climate change, whether the glacier melt can be provided sustainably and affect the agriculture, livelihood and security of the downstream region needs to be given more attention. The Western Tien Shan provided $(9.78 \pm 8.29) \times 10^8$ m^3 and $(5.38 \pm 4.83) \times 10^8$ m^3 of glacier runoff to the Weigan River basin and Aksu River basin, respectively, while providing the Ili River basin and Kai-kong River basin with $(6.03 \pm 4.39) \times 10^8$ m^3 and $(1.22 \pm 0.83) \times 10^8$ m^3, respectively. The Eastern Tien Shan provided $(2.03 \pm 1.56) \times 10^8$ m^3 to the Ili River basin and $(7.84 \pm 5.04) \times 10^8$ m^3 to the Middle Rivers basin while supplying the Turpan basin and Hami basin $(0.36 \pm 0.21) \times 10^8$ m^3 and $(0.37 \pm 0.25) \times 10^8$ m^3, respectively. Western Kunlun provided $(3.75 \pm 3.72) \times 10^8$ m^3, and Karakoram provided $(4.43 \pm 2.28) \times 10^8$ m^3 to the Yarkand River basin. The Qilian Shan in the Hexi Corridor provided $(1.98 \pm 1.21) \times 10^8$ m^3 and $(1.65 \pm 1.09) \times 10^8$ m^3 of meltwater runoff to the Shule River basin and Heihe River basin, respectively. However, neither the Eastern Kunlun nor the Qilian Shan provided less runoff to the Eastern Qaidam basin, totalling approximately $(0.04 \pm 0.04) \times 10^8$ m^3. The Kashgar River received $(2.08 \pm 1.78) \times 10^8$ m^3 of meltwater from Pamir, and the Yarkand River basin received $(0.21 \pm 0.21) \times 10^8$ m^3. The Western Qaidam Basin received a total of $(3.76 \pm 2.65) \times 10^8$ m^3 of glacial meltwater. The MK value of delayed runoff and meltwater runoff for all basins were illustrated in Extended Data Fig. 4 and 5.

3.2 Glacier Runoff validation

Some studies (Barnett et al., 2005; Hussain et al., 2019; Li et al., 2018; Wang et al., 2015; Wu et al., 2018; Yang et al., 2015; Ye et al., 2017) simulated glacial runoff in the DAC by qualitative or semi-quantitative methods or by using models. This paper used these results to verify our estimations, although there were no data in any river basins or there were only trend studies in any river basins, as shown in Fig. 4.

The upstream inflow of the Heihe River was mainly influenced by annual precipitation and glacier meltwater runoff (Jin et al., 2015). The percentage of glacier runoff recharge calculated by the DDF model was between 5% and 15% based on the first Chinese inventory and monthly precipitation and temperature data from the National Meteorological Centre (Gao et al., 2010). Wang et al. used the standardized streamflow index (SSI) and standardized precipitation evapotranspiration index (SPEI) to estimate that the percentage of glacier runoff recharge was 5.2%. Obtaining the glacier runoff recharge by comparing observations of the Yingluoxia hydrological station out of the mountain and glacier runoff, the estimation in this paper was (8.75 ± 5.83) %, which was in line with previous studies from 2004 to 2015.

In the Shiyang River basin, a previous study estimated that the glacier runoff was 0.61×10^8 m^3 from 1961 to 2006 (Gao et al., 2010), while our estimation was $(0.31 \pm 0.16) \times 10^8$ m^3, which was lower than the former. The peak glacier runoff in the Shiyang River basin occurred in the early 21st century where the proportion of meltwater runoff was close to 100% (Zhang et al., 2015). According to the MK test in this paper, the turning point of meltwater runoff in the Shiyang River basin appeared in 2000, and the meltwater runoff in the Shiyang River basin began to decline in 2000.

The Changmabao hydrological station stands out of the mountain pass in the Shule River. Li et al. calculated that glacier runoff in the Shule River basin accounted for 30.5% of the total runoff (Li et al., 2019). The average runoff growth rate of the Changmabao hydrological station in each decade from 1960 to 2015 was 1.075×10^8 m^3 (10a)$^{-1}$ according to Li's calculation and 0.91×10^8 m^3 (10a)$^{-1}$ according to Yang's calculation (Yang et al., 2017). In comparison, we found that the increase in glacier runoff in the Shule River basin was $(0.66 \pm 0.56) \times 10^8$ m^3 (10a)$^{-1}$ in this paper. By comparing the hydrological data of

Changmabao hydrological station from 2004 to 2015, the recharge rate of glacier runoff obtained in this paper was (19.21 ± 13.02) %, which was slightly lower than Li's observations.

The runoff growth rate was 2.01 × 10^8 m^3 $(10a)^{-1}$ from 1961 to 2015 based on the hydrological records of Kaqun hydrological station of the Yarkand River. The precipitation in the upper reaches of the Yarkand River changed little since 1960, with values of 640.7 mm from 1961 to 1990 and 651.9 mm from 1991 to 2006. Most of the increase was caused by glacier meltwater (Gao et al., 2010). In this paper, the meltwater runoff growth rate of the Yarkand River was calculated to be (1.87 ± 0.63) × 10^8 m^3 $(10a)^{-1}$. Zhang et al. used the DDF model to obtain values of 23.80 × 10^8 m^3 from 1961 to 1990 and 30.10 × 10^8 m^3 from 1991 to 2006 (Zhang et al., 2012). In this paper, the calculated values were (14.40 ± 4.79) × 10^8 m^3 from 1961 to 1990 and (16.92 ± 5.79) × 10^8 m^3 from 1991 to 2006. The mass balance quantities were -89.5 mm and -301.2 mm, which were both large compared with the Shean estimation (33.25 ± 210.69) mm. As the mass balance was much lower than Zhang et al., the estimations were also lower.

Using hydrological datas from Ulurawati station and Tongguzilok station in the Hotan River, the MK test showed that the runoff of the Hotan River increased at a rate of 0.084 × 10^8 m^3 a^{-1} from 1960 to 2016 (Liu, Long, et al., 2019). Based on APHRODITE, this paper found that the average rainfall in the Hotan River basin from 1961 to 2015 was 78.82 mm with no obvious change. Meanwhile, the growth rate of glacier runoff calculated in this paper was (0.078 ± 0.059) × 10^8 m^3 a^{-1}, which was similar.

Based on the monthly runoff observation data and daily meteorological data of the Weigan River basin during 1960-2013, Qin et al. studied the runoff variation of the Weigan River basin in the last 54 years and reported a value of 1.8× 10^8 m^3 $(10a)^{-1}$, of which approximately 75% was caused by glacier meltwater (Qin et al., 2016). We calculated that the growth rate of total glacier runoff in the Weigan River basin during 1961-2015 was (0.911 ± 0.671) × 10^8 m^3 $(10a)^{-1}$. A similar calculation found that the average glacier runoff in the Weigan River basin was 16.66 × 10^8 m^3, while our estimate was (12.69 ± 11.19) × 10^8 m^3 (Duan et al., 2010).

https://doi.org/10.5194/hess-2021-377
Preprint. Discussion started: 22 September 2021

Hydrology and Earth System Sciences
Discussions

Glacier runoff in the Ili River basin was calculated to be 37.18 × 10^8 m^3 (Li et al., 2010), while there was a prior different result 26.14 × 10^8 m^3 (Liu, 1999; Yang et al., 1987). On the basis of the Soil Water and Assessment Tool (SWAT), glacier runoff in Ili River basin were simulated to be 8.4 × 10^8 during 1966-1975 and 6.5 × 10^8 m^3 during 2000-2008 (Xu et al., 2015). The glacier runoff calculated in this paper was (9.16 ± 7.33) × 10^8 m^3 from 1966 to 1975 and (9.91 ± 7.83) × 10^8 m^3 from 2000 to 2008, which were in line with estimations by SWAT (Xu et al., 2015).

Using the formula of the general glacier melting model to calculate that the glacier runoff in Kai-kong River basin in the 1980s accounted for 22.1% of the total value of 33.80 × 10^8 m^3, namely, 7.47 m × 10^8 m^3, and in 2000, it accounted for 21.1% of the total value of 36.96 × 10^8 m^3, namely, 7.8 × 10^8 m^3 (Gao et al., 2008). This paper calculated that the glacial runoff in the Kai-kong River basin in the 1980s was (2.82 ± 1.92) × 10^8 m^3 and that in 2000 was (4.05 ± 2.75) × 10^8 m^3. The runoff supply rate of glacier runoff in the Kai-kong River basin was 15.2%, and that at Dashankou hydrological station was 32.94 × 10^8 m^3 during 1956-1986 and 36.96 × 10^8 m^3 during 1987-2000 (Gao et al., 2008). The supply rates calculated in this paper were (8.40 ± 5.23) % and (8.81 ± 3.58) %. Similar to the Aksu River basin, Wang et al. showed that the observations at the Xiehela hydrological station and Shaliguilanke hydrological station were 45.70 × 10^8 m^3 during 1961-1986 and 52.60 × 10^8 m^3 during 1987-2000. Wang et al. calculated that the recharge of glacier runoff in the Aksu River basin was 24.7%, while we calculated that the recharges were (17.33 ± 9.71) % and (15.35 ± 13.65) % during 1961-1986 and 1987-2000, respectively. Su et al. (2016) and Mardan et al. (2016) obtained a value of 14.60 × 10^8 m^3 for the mountainous Ebinur Drainage System in the 1980s, and we estimated that the recharge of glacier runoff was (25.19 ± 13.53)%, which was in line with 24.4% of Wang et al. (2019).

Runoff changes in the Hami Basin (including the Toudaogou Sub-Basin, Guxiang Sub-Basin, and Yushugou Sub-Basin) originating in Eastern Tien Shan from 1979 to 2007 were found that in the Guxiang Sub-Basin and Sub-Yushugou Basin with glaciers were relatively small (Wang et al., 2015), which was consistent with the trend of meltwater runoff in this paper. During the period from 1979 to 2007, the meltwater runoff in the Hami Basin had a slight decreasing trend, the rainfall had a slight increasing trend, and the overall runoff had a small change. The runoff in Western and Eastern Qaidam Basin has been increasing in the past 60 years. Wang (2019) made use of the data from 28 meteorological stations in Qinghai Province from the CMDSC and the runoff datasets of each hydrological station in Western and Eastern Qaidam Basin, combined with the MK test, and found that there was a sudden change in runoff in 2002. This result was similar to the turning point of meltwater runoff calculated in this paper (the turning point of Eastern Kunlun occurred in Western and Eastern Qaidam Basin in 2004 and 2002, and the abrupt change points of the Qilian Shan both occurred in Western and Eastern Qaidam Basin in 2001). Wang noted that temperature had a greater effect on runoff, with a correlation coefficient of 0.6**, which was similar to the increase in meltwater runoff caused by the accelerated melting of glaciers due to the increased temperature.

Our results were consistent with those of most studies. However, there was a large difference between the runoff of previous studies and that in the Yarand River basin. Because Zhang et al.'s estimation was based on glacier data with long-term observations of mass balance and obtained the mass balance trend of the whole region based on these data; however, this method was prone to cause large uncertainties. In view of the current qualitative or semi-quantitative analysis of the influence of glaciers on runoff, quantitative research on glacial meltwater is very scarce, which brings strong uncertainty to the future prediction of different basins. The model established in this paper could provide a new approach for the prediction of glacier runoff in the future. Of course, field observation is the most accurate method to study glaciers, and the establishment of observation systems and continuous hydrological monitoring based on different types and areas of glaciers could further and more accurately predict the evolution of glaciers and glacial water sources.

https://doi.org/10.5194/hess-2021-377
Preprint. Discussion started: 22 September 2021

Hydrology and Earth System Sciences
Discussions
Open Access

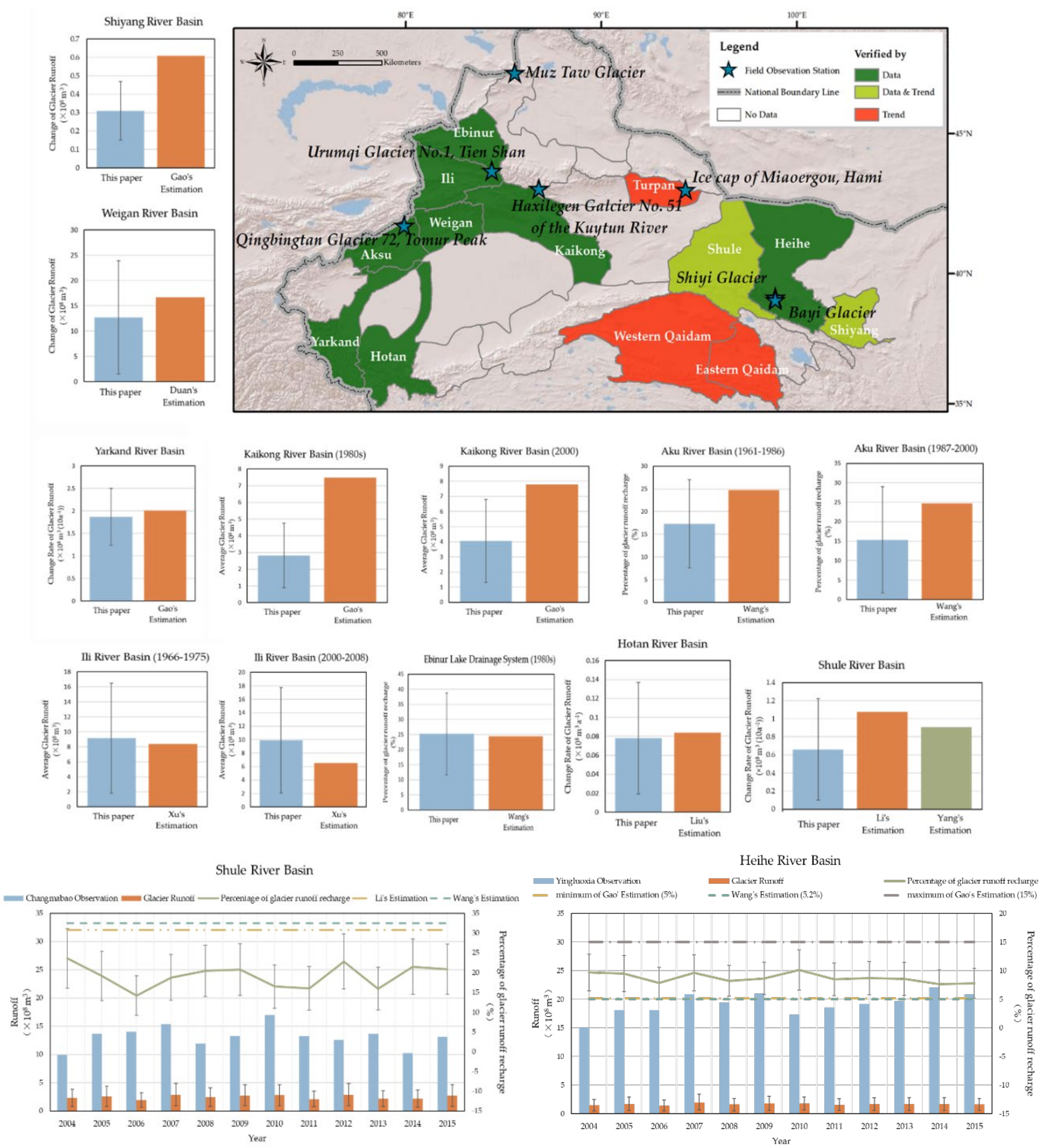

431 **Fig. 4. Map of glacier runoff validation.** Some basins had relevant data verification, some basins had both data and trend verification, some basins had only trend verification, and the areas without color lacked data. The study on glacier runoff in the DAC was unevenly distributed. The blue color in each chart was the glacier runoff calculated in this paper, and the other colors represented runoff obtained in different studies. World Shaded Relief provided by Esri (http://goto.arcgisonline.com/maps/World_Shaded_Relief).

3.2 Glacier Classification Based on Potential Climatic Risks

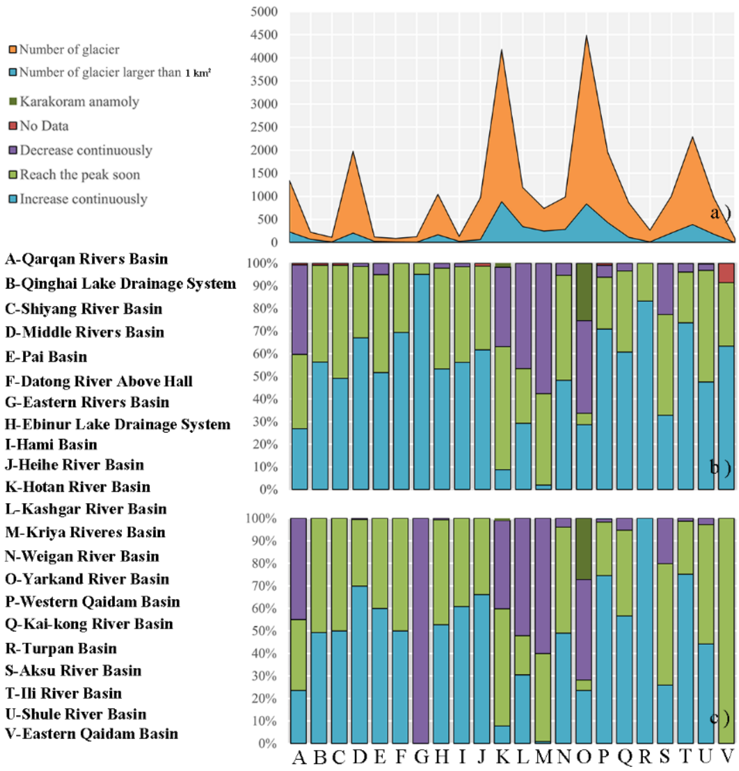

Fig. 5. Statistical maps of different types and quantities of glaciers in each basin. a) Stacked area chart of the number of glaciers and glaciers larger than 1 km^2. b) Stacked bar chart of different types of glaciers under future changes. c) Stacked bar chart of different types of glaciers larger than 1 km^2 under future changes.

Based on the time series of glacier runoff, linear regression was used to predict the runoff of each glacier in DAC in the next decade as shown in Fig. 5. The Hotan River Basin, Yarkand River Basin and Ili River Basin in Xinjiang Province contained more than 2,000 glaciers according to RGI. Glaciers larger than 1 km^2 were more stable in the face of potential climate change risks while the number of glaciers larger than 1 km^2 was strongly consistent with the total number of glaciers contained in the basin. In the next ten years, the runoff of most basins would continue to increase, including the Qinghai Lake Drainage System, Eastern Rivers Basin, Turpan Basin and Eastern Qaidam Basin. Linking "Reach the peak soon" and "Decrease continuously", the Hotan River Basin, and Kashgar River Basin and Kriya Rivers Basin where delayed runoff accounted for larger glacier

https://doi.org/10.5194/hess-2021-377
Preprint. Discussion started: 22 September 2021

runoff were affected by potential climatic risks over the next decade. Qarqan Rivers Basin and Kai-kong River Basin would also reduce by potential climatic risks. Focusing on glaciers larger than 1 km^2 revealed a reversal. In the Eastern Rivers Basin, the glaciers larger than 1 km^2 would basically continue to decline in the next ten years, contrary to the overall trend of rising glacier meltwater runoff. Different from other continental glaciers, a significant area of glaciers in Karakoram remained relatively stable, which was called "Karakoram anomaly". Therefore, both larger than 1 km^2 and other smaller glacier in the Yarkand River Basin would remain the anomalous relatively stable in the face of potential climate risks in the next decade.

3.4 The Spatiotemporal Change in Glacier Runoff

MK test values of glacier runoff in all basins were shown in Fig. 6. The ratio called the change rate of the coefficient obtained by the least square linear regression to the mean value of glacier runoff in each basin during 1965-2015 was combined with the results of the MK test to determine the temporal change trend of glacier runoff in each basin, as shown in Fig. 7. According to the MK test value and the change rate, the glacier runoff in the Shiyang River basin showed a declining trend and decreased significantly in 2010, which made the basin the most unique among all the basins, while the MK test showed that glacier runoff in the Datong River above Hall was more likely to fluctuate. The trend of the change rate between 0 and 0.3 was determined as a weak fluctuation, i.e., there was no obvious trend of increase or decrease in regions including the Shule River basin, Qinghai Lake Drainage System, Pai Basin, Hami Basin, Weigan River basin and Aksu River basin, where change trends were also not significant. A change rate greater than 0.3 indicated a strong increasing trend. There was an abrupt change in the MK test value in the Middle Rivers basin, Eastern Rivers basin, Turpan Basin and Kashgar River basin in 2006, 2006, 2007 and 1990, respectively, rather than a stable increasing trend. Therefore, this paper listed the trend of these four basins as "fluctuated and increased" based on the MK tests, but the trends were not significant. Glacier runoff in basins such as the Hotan River basin, Yarkand River basin, Kriya Rivers basin, Qarqan Rivers basin, Western Qaidam Basin, Eastern Qaidam Basin, Ili River basin, Ebinur Lake Drainage System and Kai-kong River basin showed gradual increasing trends from 1961 to 2015, although the trends became significant at different times in different basins.

https://doi.org/10.5194/hess-2021-377
Preprint. Discussion started: 22 September 2021

The average change rate in all basins affected by glaciers in the DAC was 0.48%. Although most of the river basins showed increasing trends and reached significance at different time points, the reasons for the sudden increase in the basins classified as “fluctuating and increasing” were not clear. The river basins originating from the Qilian Shan, such as the Shule River basin, Qinghai Lake Drainage System, Heihe River basin and Datong River above Hall, showed weak increasing or fluctuating trends, which indicated that the supply of glacier runoff in the Qilian Shan was relatively stable, while the decline in glacier runoff in the Shiyang River basin sounded an alarm. Persistently affected by climate change, it was difficult to determine how much glacier runoff could be provided in the next few years.

https://doi.org/10.5194/hess-2021-377
Preprint. Discussion started: 22 September 2021

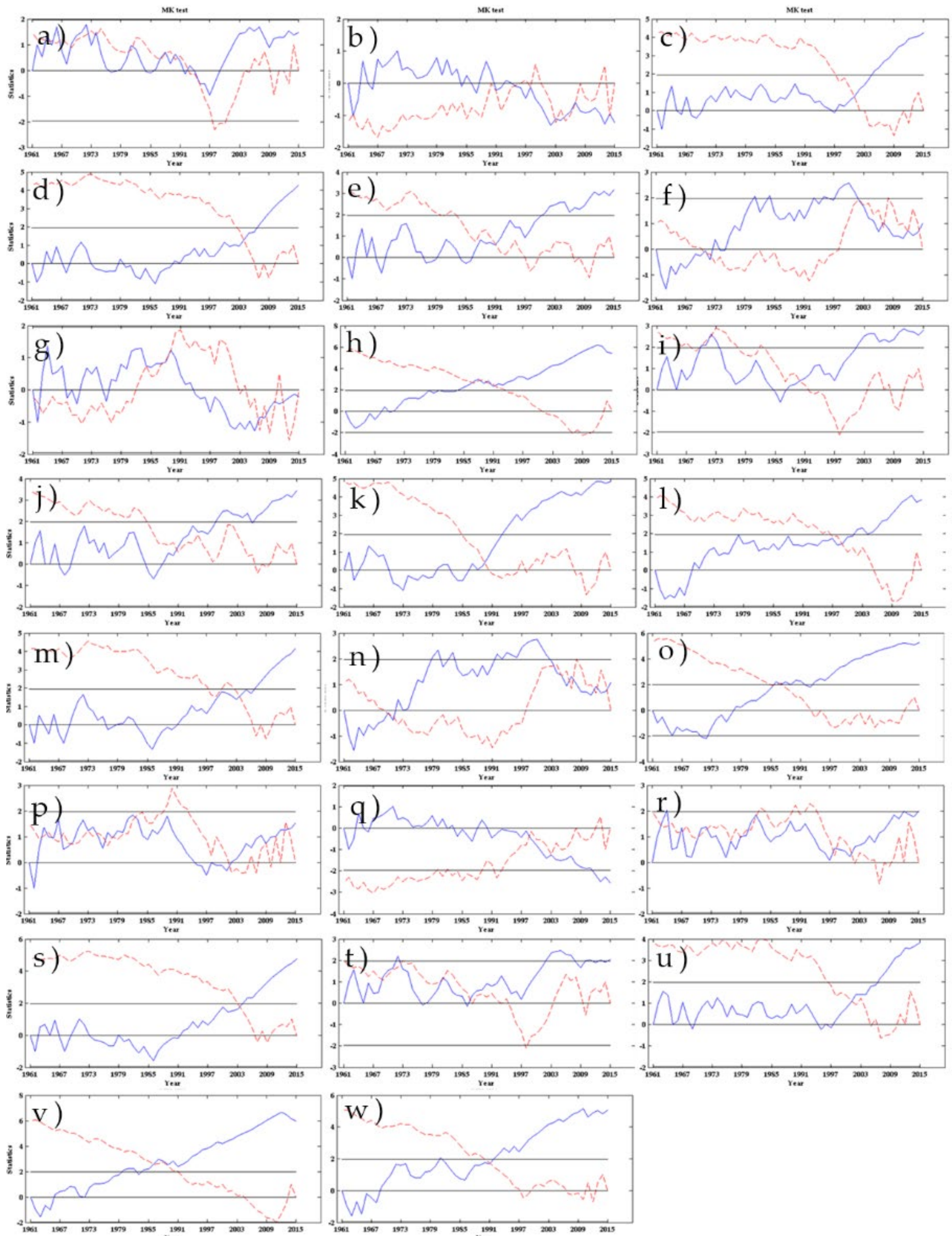

478 **Fig. 6. Mann-Kendall Test of total glacier runoff with a confidence of 95%** in a)Aksu River Basin, b)Datong River
479 Above Hall, c)Eastern Qaidam Basin, d)Eastern Rivers Basin, e)Ebinur Lake Drainage System, f)Hami Basin, g)Heihe
480 River Basin, h)Hotan River Basin, i)Ili River Basin, j)Kai-kong River Basin, k)Kashgar River Basin, l)Kriya Rivers
481 Basin, m)Middle Rivers Basin, n)Pai Basin, o)Qarqan Rivers Basin, p)Qinghai Lake Drainage System, q)Shiyang River

https://doi.org/10.5194/hess-2021-377
Preprint. Discussion started: 22 September 2021

Hydrology and Earth System Sciences
Discussions

Basin, r)Shule River Basin, s)Turpan Basin, t)Weigan River Basin, u)Western Qaidam Basin, v)Yarkand River Basin, w)Entire Basins. **Blue line referred to the UF curve and red line referred to the UB curve and the lines at ± 2 represented a 95% confidence interval**. While $UF > 0$, it indicated an increasing trend of the sequence, on the contrary, it indicated a declining trend while $UF < 0$. The year UF curve intersected the UB curve in the confidence interval was determined as the turning year.

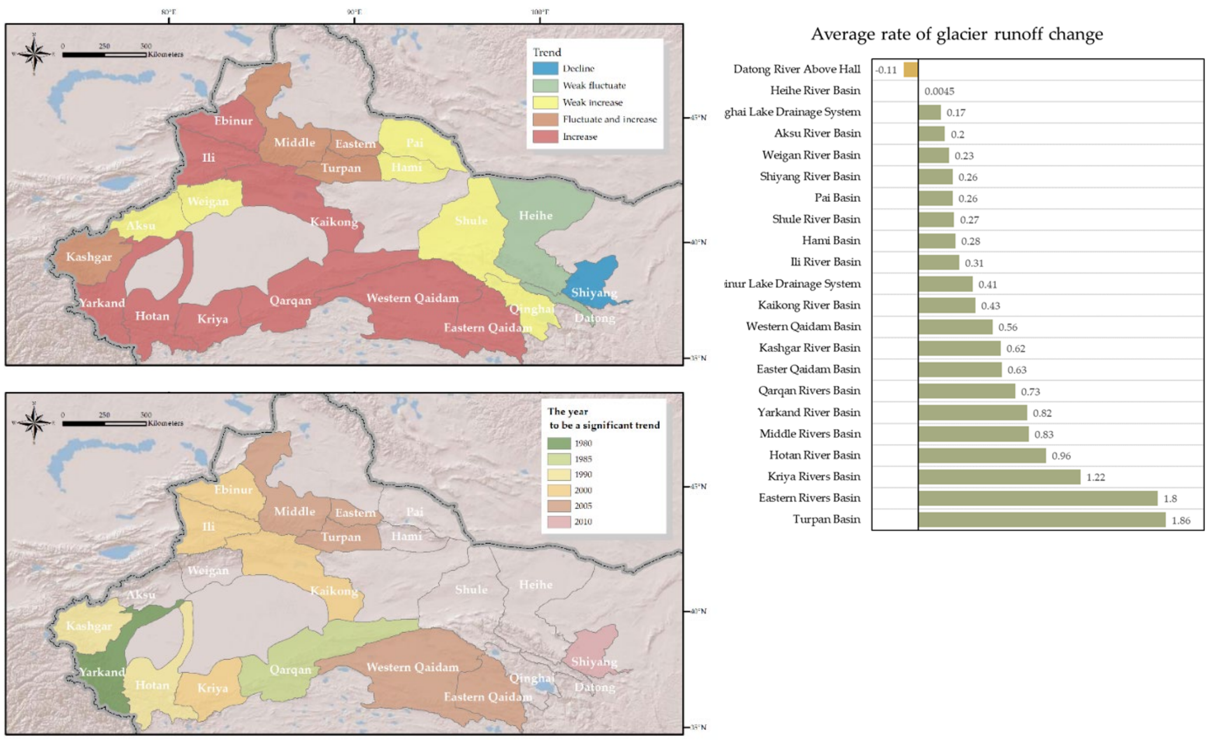

Fig. 7. Spatiotemporal regime of glacier runoff in the DAC. a) the trend of glacier runoff, b) the year with a significant trend, and c) the average rate of glacier runoff change. The trends classified as "weak fluctuating" and "weak increase" had no significant time. Except for Shiyang River basin and Datong River above Hall, glacier runoff increased from 1961 to 2015. World Shaded Relief provided by Esri (http://goto.arcgisonline.com/maps/World_Shaded_Relief).

https://doi.org/10.5194/hess-2021-377
Preprint. Discussion started: 22 September 2021

4 Discussion

4.1 Precipitation Correction at High-altitudes

Some glaciology studies believed that two maximum rainfall heights could appear on one high mountain. For example, the Chinese Academy of Sciences (CAS) established eight rainfall observation points in the middle part of Tien Shan in 1959 and observed that maximum rainfall heights occurred at two altitudes, 1850 m and 5339 m (Zhang, Tuerxunbai, et al., 2019; Zhao et al., 2011). The same institute placed observation points in western Tien Shan in 1978 and found that the first maximum rainfall height was 2400 m, and the second was 3200 m (Kou & Su, 1981). A study on the change in precipitation with altitude in the Qilian Shan showed that the precipitation in coteau presented an "S" type distribution with increasing altitude (Tang, 1985). The second maximum rainfall height was believed to exist by studies on Tien Shan, North Slope of Karakoram, which is located in the alpine glacier region (Shen & Liang, 2006).

Table 2. H_{map} and H_{max} used in this paper. H_{map} in Eastern Kunlun and Western Kunlun were speculated by five other regions that had references about maximum rainfall height. H_{max} refers to the average of the maximum height of each glacier in regions of RGI 6.0.

Region	H_{map}	H_{max}
Qilian Shan	4200 (et al., 2018; Wang et al., 2009)	5500
Eastern Tien Shan	3000 (Zhang, Tuerxunbai, et al., 2019)	5000
Western Tien Shan	3000 (Zhang, Tuerxunbai, et al., 2019)	6000
Eastern Kunlun	4500	6500
Western Kunlun	4000	6500
Karakoram	2500 (Immerzeel et al., 2012)	7500
Pamir	3000 (Hewitt, 2007)	6500

However, other meteorological studies believed that there was only one maximum rainfall height on one high mountain because when the elevation was above the maximum rainfall height, the airflow continued to rise, but the water vapor rapidly decreased and the precipitation could not increase again generally. Some research (Immerzeel et al., 2015) took the maximum rainfall height as the reference height and believed that the average maximum rainfall height in the Indus River basin was 2500 m when calculating the precipitation on the glacier (Hewitt, 2007; Immerzeel, et al., 2012). Putkonen (2004) calculated that the maximum rainfall height on the Southern Slope of the Himalayas was approximately 3000 m, while a subsequent calculated that the maximum rainfall height zone on the July 1 glacier of the Qilian Shan was located at 4500-4700 m (Wang et al., 2009).

There has always been controversy over whether there is one or two maximum altitudes in the mountains. Even in the same region, there are different results due to the limitations of the discipline, purpose, method, time or initial conditions of the study. Zhao et al. (2011) thought there was only a maximum rainfall height in the Northern Slope of Tien Shan, and a subsequent study which was by dividing the elevation zones by 100 m using TRMM, found that rainfall in Tien Shan peaked at an annual level of 3500 m even though zones were divided into different geomorphic units (Bai et al., 2017). The results of Bai et al. (2017) were different from those of the CAS in 1959 (3500 m vs. 1850 m and 5339 m). Additionally, observed at Gongga Shan, Zhang found that there were two maximum rainfall heights, one at 3500-4000 m and the other at 5000 m (Zhang, 2012). However, Thomas observed that there was only one maximum rainfall height at Gongga Shan, which existed at 2900-3200 m (Thomas, 1997).

The maximum rainfall height was related to the data. In the Junggar Basin, APHRODITE showed a maximum rainfall height at 4200 m, while IMAGE showed a maximum height at 2600 m. The two maximum rainfall heights of ITPCAS were at 2810 m and 4260 m. PERSIANN and TRMM showed two maximum rainfall heights, which were both at 2600 m and 4200 m. In the Turpan Basin and Hami Basin, APHRODITE, TRMM and ITPCAS all showed two maximum rainfall heights, at 2740 m and 3800 m. There were two precipitation heights of APHRODITE in the Northern Tarim Basin: 2400-3100 m and 3600-4500 m. However, there was only one maximum rainfall height using IMAGE, which was at 4000-4800 m (Zhang, 2020).

The maximum rainfall height was also related to the season. Previous research divided Xinjiang into different altitude zones according to meteorological stations' elevations, obtaining the regional variation characteristics of precipitation change with changing altitude; specifically, that in summer was 3900-4200 m, that in autumn was 3000-4000 m, and that in winter was less than 2360 m. Bai et al. believed that the maximum rainfall height in summer on the Northern Slope of Tien Shan would be

1900-2300 m, that in winter would be 900-1300 m, and the average rainfall height was approximately 3000 m (Zhang, Tuerxunbai, et al., 2019).

Fog, dew, frost and other weather phenomena are also known as horizontal precipitation, which can be seen year round in mountainous areas, especially at elevations greater than 3500 m. After condensation, this water vapor could be accepted only by the underlying surface but could not be captured by the common rain gauges commonly used for meteorological observations. Whether a rain gauge records precipitation in the high mountains correctly or not directly affects the correction of precipitation in mountainous areas. In this paper, PG was calculated according to the regional average H_{map}, so this paper used H_{map} as the standard for calculation. Bothe the H_{map} and the H_{max} are shown in Table 2.

4.2 Distribution of High-altitude Precipitation Gradient

Our estimation revealed a strong heterogeneity of the median precipitation gradient in glaciers near the DAC, as shown in Fig 8. The median precipitation gradient for the seven glacier zones was -0.0347% m^{-1}, which meant that according to H_{max} and H_{ref}, precipitation decreased by 0.0347% for every 1 m increase in elevation. The median precipitation gradients in Karakoram, Eastern Kunlun, and Eastern Tien Shan (-0.0064% m^{-1}, 0.0011% m^{-1}, and -0.0062% m^{-1}, respectively) were obviously greater than the median precipitation gradients in Eastern Kunlun, Eastern Tien Shan, Qilian Shan, and Pamir (-0.0223% m^{-1}, -0.0722% m^{-1}, -0.0999% m^{-1}, and -0.0025% m^{-1}, respectively). We found that the median precipitation gradients of glaciers in the western part of the DAC were larger than those in the eastern part; for example, the median precipitation gradient of Western Kunlun was larger than that of Eastern Kunlun, similar to the relationship between Western Tien Shan and Eastern Tien Shan. Precipitation decreased by 9.9% for every 100 m increase in elevation from the maximum rainfall height in the Qilian Shan, and precipitation increased by 0.11% for the same increases in elevation in Eastern Kunlun.

https://doi.org/10.5194/hess-2021-377
Preprint. Discussion started: 22 September 2021

Hydrology and Earth System Sciences
Discussions

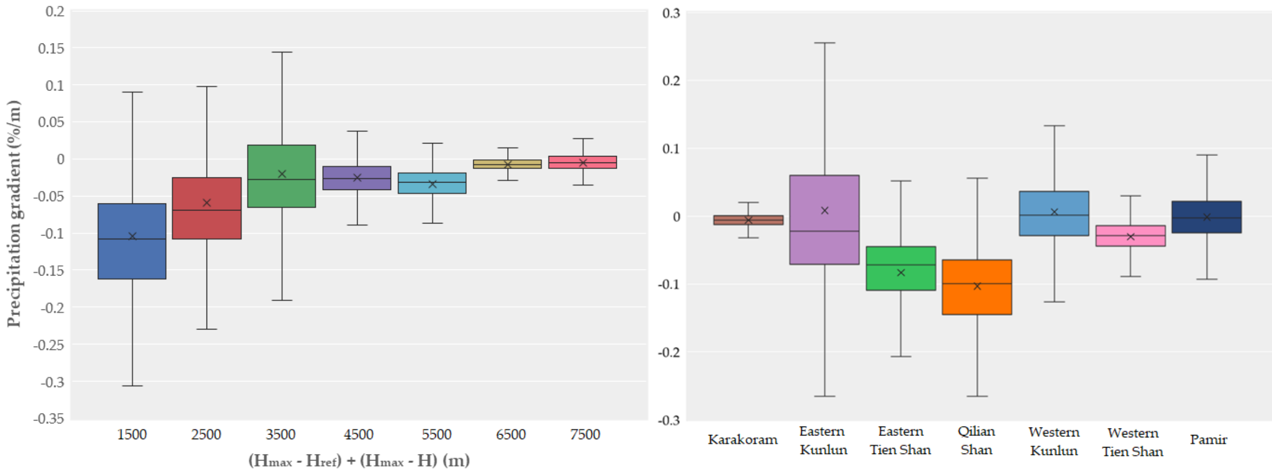

Fig. 8. Box plots of precipitation gradients for $\Delta H + (H_{max} - H)$ (m) and each glacier region. Line: median; multiple sign: average number; box: 25–75% of the observations; whiskers: min and max non-outliers.

To better understand the distribution of precipitation gradients of glaciers around the DAC, the relationship between precipitation and ΔH, which is the difference between the maximum elevation and the maximum rainfall height, was analyzed in this paper. ΔH had the largest number of glaciers between 3000 m and 4000 m, with a median PG of -0.0276% m^{-1} and a large range of maximum and minimum values. The ΔH between 6000 m and 8000 m had the highest median PG (-0.0078% m^{-1} and -0.0055% m^{-1}), which was consistent with the suggestions that the higher the tropospheric height was, the stronger the interaction between altitude and precipitation of this precipitation type was. The fewest glaciers were located in the ranges of 1000 m to 2000 m and 5000 m to 6000 m, with median PGs values of -0.1084% m^{-1} and -0.0319% m^{-1}, respectively. With the increase in ΔH, the median PG had a significant increase range at elevations of 1000 m to 4000 m, and the median PG increased by 0.0269% for every 1000 m increase in elevation.

4.3 Impact Factors

Some results have shown that both temperature and precipitation have increased significantly in the last 60 years, while the increasing trends have even obviously intensified (Javed et al., 2021; Zhang et al., 2021). The long-term trends and interannual changes in temperature and precipitation dominated the climate humidification change. While continental glaciers are sensitive

https://doi.org/10.5194/hess-2021-377
Preprint. Discussion started: 22 September 2021

to a combination of temperature (Wang et al., 2019), precipitation and snow/rain differentiation, temperature and precipitation were major factors of glacier runoff change. Changes in temperature and precipitation could change the glacier mass balance by affecting the displacement of the ELA, leading to changes in glacier areas and runoff. Previous studies have shown that the range of glacier change is larger in wetter mountains, such as Eastern Qilian Shan and the Western Tien Shan, while the range of glacier change decreases with the distance from a water vapor supply source. Most studies also showed that temperature played a leading role in hydrothermal conditions, while precipitation played a weaker role (Azam & Srivastava, 2020; Ban et al., 2020; Baojuan et al., 2020; Noel et al., 2020).

4.4 Socio-economic Consequences

OAA in the DAC relied most on glacier delayed runoff and meltwater runoff to irrigate and maintain agriculture as well as to maintain soil moisture, vegetation growth and groundwater replenishment to maintain food security (Bury et al., 2013; Clouse et al., 2016; Rasul & Molden, 2019). The 22 glacier basins in the DAC have irrigated 143,939.24 km^2 of OAA, supplying a total of 14 million people in 19 regions. The primary industry gross domestic product (GDP) of these regions in 2015 was nearly 111.54 billion dollars, accounting for 14.1% of the total GDP of these regions, which was twice that of the primary industry, accounting for 7% of the national GDP. Since the total primary industry GDP of the entire north western DAC was 40.46 million dollars, OAAs constituted 79.86% of it. Increasing glacier runoff could provide more water for agriculture and animal husbandry to ensure food security and purvey water for residential and industrial use, but the trend could not be sustained (Wang et al., 2021).

The proportion of glacier runoff in agricultural, industrial and municipal water consumption in each basin in the DAC was shown in Fig. 9. The agricultural water consumption at the watershed scale was obtained by averaging the agricultural water consumption statistical data to the land use types of agricultural land and then ranged regional statistics, which was the same with industrial and municipal water consumption. Compared with the industrial and municipal water consumption in each basin, the delayed runoff and meltwater runoff were both higher than the total industrial and municipal water consumption in this basin. Glacier runoff from the Middle Rivers Basin and Western Qaidam Basin could even provide the entire agricultural

https://doi.org/10.5194/hess-2021-377
Preprint. Discussion started: 22 September 2021

water consumption over the entire basin. When the ELA was higher than the altitude of the glacier itself, glacier runoff began to decrease, which might have adverse effects on downstream agriculture, animal husbandry, energy and livelihood. For example, due to increased temperatures and reduced glacier runoff, California, in the United States, experienced a severe drought from 2011 to 2015, where hydroelectric power generation decreased by two-thirds. The annual ecological service value in Tien Shan was 60.2 billion yuan (~9.26 billion dollars) (Zhang, Liu, et al., 2019), and that in Qilian Shan was 24.354 billion yuan (~ 3.75 billion dollars) (Sun et al., 2020). Glaciers such as the Urumqi No. 1 Glacier and July 1 Glacier in Qilian Shan have been developed as scenic plots to attract more tourists to the local area and increase the income of local residents. However, with the rise of the ELA, to protect the Urumqi No. 1 Glacier, the tourist service had been cancelled. In the future, glacier runoff will reach its peak when glacier tourism disappears (Warren & Lemmen, 2014). Even in some places, the water shortage caused by the reduction of glacier runoff has caused the risk of water pollution and the production of water-borne pathogens (Warren & Lemmen, 2014). In a study of the public perception of changes in the cryosphere in the Urumqi River basin, 58.8% of the interviewees believed that as glacial runoff increased, income also increased (Deng et al., 2011). As quantifying the economic and social impact of changes in the cryosphere is essential for making public policies and influencing adaptation decisions, our estimations could support a quantified long-term time-series glacier runoff to be referred.

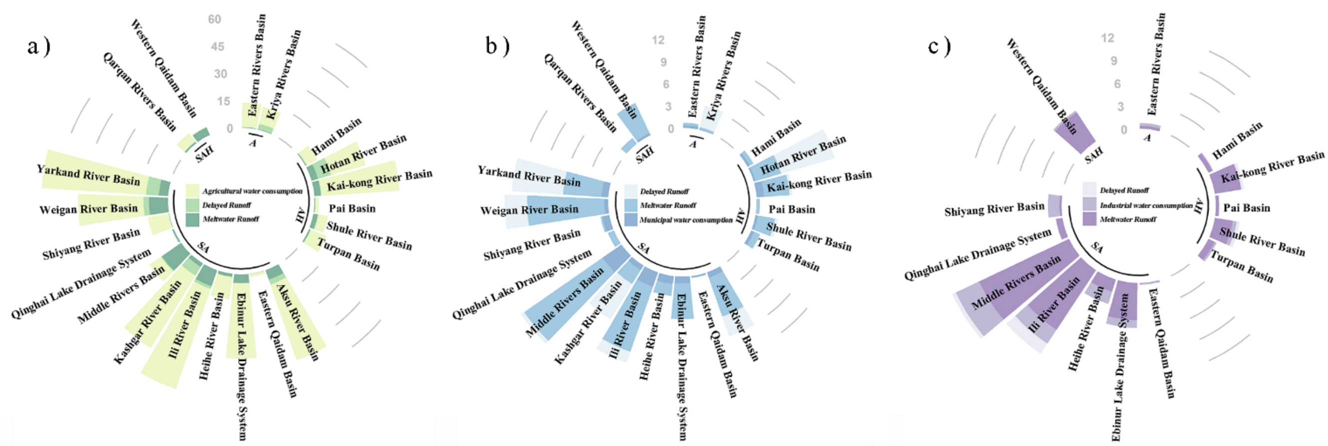

Fig. 9. Proportion of delayed runoff and meltwater runoff to a) agricultural water consumption, b) municipal water consumption and c) industrial water consumption.

5 Conclusion

This paper overcame the shortcomings of large-scale geodetic quality assessments. We used the Shean estimation and calculated the precipitation gradient to quantitatively study the seven major glacier regions around the DAC, which consisted of nearly 42,000 glaciers. The spatiotemporal changes in glacier runoff (delayed runoff and meltwater runoff) in OAAs located in 22 glacier watersheds with a spatial resolution of 100 m from 1961 to 2015 were established.

1. This paper used the mass balance of the Shean estimation to obtain a high-altitude precipitation gradient with uncertainties and then calculated the long-term time series of glacier runoff, including delayed runoff and meltwater runoff, while the average total glacier runoff in the DAC was $(98.52 \pm 67.37) \times 10^8$ m^3. The average meltwater runoff was $(63.43 \pm 42.17) \times 10^8$ m^3, and the delayed runoff was $(35.09 \pm 25.20) \times 10^8$ m^3.

2. Among all glacier watersheds, the Shiyang River basin was the most unique, which suggested a declining trend from 1961 to 2015. The Datong River above Hall and the Heihe Basin showed fluctuating trends, while the others showed different growth trends. Based on the time series of glacier runoff, linear regression was used to predict the runoff of each glacier in DAC in the next ten years which indicated the potential climatic risks.

3. As a continental glacier, the glacier runoff studied in this paper was mainly regulated by hydrothermal regulation, in which temperature was the dominant factor, followed by precipitation. Since the water source of the oases in the DAC was mostly glaciers and the total GDP of the OAAs accounted for 76.92% of that of the north western DAC, glacier runoff had a greater impact on local agriculture, animal husbandry, and economy. In the future, it is necessary to quantify the impact of each change in the cryosphere on social production factors more precisely.

References

Adler, C., Huggel, C., Orlove, B., and Nolin, A.: Climate change in the mountain cryosphere: impacts and responses, Reg. Environ. Change., 19, 1225-1228, doi: 10.1007/s10113-019-01507-6, 2019.

Arora, N. K., & Mishra, I.: United Nations Sustainable Development Goals 2030 and environmental sustainability: race against time, Environ. Sustainability, 2, 339-342, doi: 10.1007/s42398-019-00092-y, 2019.

Avtar, R., Aggarwal, R., Kharrazi, A., Kumar, P., and Kurniawan, T. A.: Utilizing geospatial information to implement SDGs and monitor their Progress, Environ. Monit. Assess., 192, 35, doi: 10.1007/s10661-019-7996-9, 2019.

Azam, M. F., and Srivastava, S.: Mass balance and runoff modelling of partially debris-covered Dokriani Glacier in monsoon-dominated Himalaya using ERA5 data since 1979, J. Hydrol., 590, doi: 10.1016/j.jhydrol.2020.125432, 2020.

Azam, M. F., Wagnon, P., Ramanathan, A., Vinicent, C., Sharma, P., Arnaud, Y., Linda, A., Pottakkal, J. G., Chevallier, P., Singh, V. B., and Berthier, E.: From balance to imbalance: a shift in the dynamic behaviour of Chhota Shigri glacier, western Himalaya, India, J. Glaciol., 58, 315-324, doi: 10.3189/2012JoG11J123, 2012.

Ban, C., Xu, Z., Zuo, D., Liu, X., Zhang, R., and Wang, J. (2020): Vertical influence of temperature and precipitation on snow cover variability in the Yarlung Zangbo River basin, China, Int. J. Climatol., 41, 1148-1161, doi: 10.1002/joc.6776, 2020.

Baojuan, H., Weijun, S., Junyao, W., Yetang, W., Zhongqin, L., and Hui, Z.: A long glacier mass balance record analysis in Chinese Urumqi Glacier No. 1 and the relationships with changes in large-scale circulations, Arabian J. Geosci., 13, doi: 10.1007/s12517-020-06224-7, 2020.

Barnett, T. P., Adam, J. C., and Lettenmaier, D. P.: Potential impacts of a warming climate on water availability in snow-dominated regions, Nature, 438, 303-309, doi: 10.1038/nature04141, 2005.

Beniston, M., and Stoffel, M.: Assessing the impacts of climatic change on mountain water resources, Sci. Total Environ., 493, 1129-1137, doi: 10.1016/j.scitotenv.2013.11.122, 2014.

Bibi, S., Wang, L., Li, X., Zhou, J., Chen, D., and Yao, T.: Climatic and associated cryospheric, biospheric, and hydrological changes on the Tibetan Plateau: a review, Int. J. Climatol., 38, e1-e17, doi: 10.1002/joc.5411, 2018.

Bie, Q., and Xie, Y.: The constraints and driving forces of oasis development in arid region: a case study of the Hexi Corridor in northwest China, Scientific Reports, 10, 17708, doi: 10.1038/s41598-020-74930-z, 2020.

Biemans, H., Siderius, C., Lutz, A. F., Nepal, S., Ahmad, B., Hassan, T., von Bloh, W., Wijngaard, R. R., Wester, P., Shretha, A. B., Immerzeel, W. W.: Importance of snow and glacier meltwater for agriculture on the Indo-Gangetic Plain, Nat. Sustain., 2, 594-601, doi: 10.1038/s41893-019-0305-3, 2019.

Bolch, T., Shea, J. M., Liu, S., Azam, F. M., Gao, Y., Gruber, S., et al. (2019). Status and Change of the Cryosphere in the Extended Hindu Kush Himalaya Region. In P. Wester, A. Mishra, A. Mukherji, & A. B. Shrestha (Eds.), The Hindu Kush Himalaya Assessment: Mountains, Climate Change, Sustainability and People (pp. 209-255). Cham: Springer International Publishing. http://doi.org/10.1007/978-3-319-92288-1

Braithwaite, R. J. and Olesen, O. B.: Seasonal variation of ice ablation at the margin of the Greenland ice sheet and its sensitivity to climate change, Qamanârssûp sermia, West Greenland, J. Glaciol., 39, 267-274, doi: 10.3189/S0022143000015938, 1993.

Brun, F., Berthier, E., Wagnon, P., Kääb, A., and Treichler, D.: A spatially resolved estimate of High Mountain Asia glacier mass balances from 2000 to 2016, Nat. Geosci., doi: 10, 668-673, 10.1038/ngeo2999, 2017.

Bury, J., Mark, B. G., Carey, M., Young, K. R., McKenzie, J. M., Baraer, M., French, A., and Polk, M. H.: New Geographies of Water and Climate Change in Peru: Coupled Natural and Social Transformations in the Santa River Watershed, Ann. Assoc. Am. Geogr., 103, 363-374, doi: 10.1080/00045608.2013.754665, 2013.

Chen, R., Han, C., Liu, J., Yang, Y., Liu, Z., Wang, L., and Kang, E.: Maximum precipitation altitude on the northern f lank of the Qilian Mountains, northwest China, Hydrol. Res., 49, 1696-1710, doi: 10.2166/nh.2018.121, 2018.

Chen, Y., Li, W., Deng, H., Fang, G., and Li, Z.: Changes in Central Asia's Water Tower: Past, Present and Future, Sci. Rep., 6, 35458, doi: 10.1038/srep35458, 2016.

Clouse, C., Anderson, N., and Shippling, T.: Ladakh's artificial glaciers: climate-adaptive design for water scarcity, Clim. Dev., 9, 428-438, doi: 10.1080/17565529.2016.1167664, 2017.

Compagno, L., Eggs, S., Huss, M., Zekollari, H., and Farinotti, D.: Brief communication: Do 1.0, 1.5, or 2.0 °C matter for the future evolution of Alpine glaciers?, Cryosphere, 15, 2593-2599, doi: 10.5194/tc-15-2593-2021, 2021.

Deng, M., Zhang, H., Mao, W., and Wang, Y.: Public Perceptions of Cryosphere Change and the Selection of Adaptation Measures in the Ürümqi River Basin, Adv. Clim. Chang. Res., 2, 149-158, doi: 10.3724/SP.J.1248.2011.00149, 2011.

Ding, Y., Liu, S., Li, J., and Shangguan, D.: The retreat of glaciers in response to recent climate warming in western China, Ann. Glaciol., 43, 97-105, doi: 10.3189/172756406781812005, 2006.

Duan, J. J., Cao, X. L., Shen, Y. P., Gao, Q. Z., and Wang, S. D.: Surface Water Resources and Its Trends in Weigan River Basin on the South Slope of Tianshan, China during 1956-2007, J. Glaciol. Geocryol. (in Chinese), 32, 1211-1219, doi: 10.7522/j.issn.1000-0240.2010.06.1211.09, 2010.

Duan, Y. Y., Liu, T., Meng, F., Yuan, Y., Luo, M., Huang, Y., Xing, W., Nzabarinda, V., and De Maeyer, P.: Accurate Simulation of Ice and Snow Runoff for the Mountainous Terrain of the Kunlun Mountains, China, Remote Sens., 12, 179, doi: 10.3390/rs12010179, 2020.

Fan, Y., Chen, Y., Liu, Y., and Li, W.: Variation of baseflows in the headstreams of the Tarim River Basin during 1960–2007, J. Hydrol., 487, 98-108, doi: 10.1016/j.jhydrol.2013.02.037, 2013.

Fujita, K. and Nuimura, T.: Spatially heterogeneous wastage of Himalayan glaciers, P. Natl. Acad. Sci. USA, doi: 108, 14011, 10.1073/pnas.1106242108, 2011.

Gao, Q. Z., Wang, R., and Giese, E.: Impact of Climate Change on Surface Runoff of Tarim River Originating from the South Slopes of the Tianshan Mountains, J. Glaciol. Geocryol. (in Chinese), 30, 1-11, doi: 10.7522/j.issn.1000-0240.2008.01.0001.11, 2008.

https://doi.org/10.5194/hess-2021-377
Preprint. Discussion started: 22 September 2021

Gao, X., Zhang, S. Q., Ye, B. S., and Qiao, C. J.: Glacier Runoff Change in the Upper Stream of Yarkand River and Its Impact on River Runoff during 1961-2006, J. Glaciol. Geocryol. (in Chinese), 32, 445-453, doi: 10.7522/j.issn.1000-0240.2010.03.0445.09, 2010.

Garee, K., Chen, X., Bao, A., Wang, Y., and Meng, F.: Hydrological Modeling of the Upper Indus Basin: A Case Study from a High-Altitude Glacierized Catchment Hunza, Water, 9, doi: 10.3390/w9010017, 2017.

Georg, G. and William, S. K.: Mountain Forests and Sustainable Development: The Potential for Achieving the United Nations' 2030 Agenda, Mt. Res. Dev., 37, 246-253, doi: 10.1659/MRD-JOURNAL-D-17-00093.1, 2017.

Guan, X., Zhang, J., Yang, Q., Tang, X., Liu, C., Jin, J., Liu, Y., Bao, Z., and Wang, G.: Evaluation of Precipitation Products by Using Multiple Hydrological Models over the Upper Yellow River Basin, China, Remote Sens., 12, doi： 10.3390/rs12244023, 2020.

Han, Z., and Zhou, T.: Assessing the Quality of APHRODITE High-Resolution Daily Precipitation Dataset over Contiguous China. Chin. J. Atmos. Sci. (in Chinese), 36, 361-373, doi: 10.3878/j.issn.1006-9895.2011.11043, 2012.

Hausner, V. H., Engen, S., Brattland, C., and Fauchald, P.: Sámi knowledge and ecosystem-based adaptation strategies for managing pastures under threat from multiple land uses, J. Appl. Ecol., 57, 1656-1665, doi: 10.1111/1365-2664.13559, 2020.

Hewitt, K.: Tributary glacier surges: an exceptional concentration at Panmah Glacier, Karakoram Himalaya, J. Glaciol., 53, 181-188, doi: 10.3189/172756507782202829, 2007.

Hinz, R., Sulser, T. B., Huefner, R., Mason-D'Croz, D., Dunston, S., Nautiyal, S., Ringler, C., Schuengel, J., Tikhile, P., Wimmer, F., and Schaldach, R.: Agricultural Development and Land Use Change in India: A Scenario Analysis of Trade-Offs Between UN Sustainable Development Goals (SDGs), Earth's Future, 8, e2019EF001287, doi: 10.1029/2019EF001287, 2020.

Huang, X., Sillanpää, M., Gjessing, E. T., and Vogt, R. D.: Water quality in the Tibetan Plateau: Major ions and trace elements in the headwaters of four major Asian rivers, Sci. Total Environ., 407, 6242-6254, doi: 10.1016/j.scitotenv.2009.09.001, 2009.

Hussain, D., Kuo, C.-Y., Hameed, A., Tseng, K.-H., Jan, B., Abbas, N., Kao, H.-C., Lan, W.-H., and Imani, M.: Spaceborne Satellite for Snow Cover and Hydrological Characteristic of the Gilgit River Basin, Hindukush-Karakoram Mountains, Pakistan, Sensors, doi: 19, 531, 10.3390/s19030531, 2019.

Immerzeel, W. W. and Bierkens, M. F. P.: Asia's water balance, Nat. Geosci., 5, 841-842, doi: 10.1038/ngeo1643, 2012.

Immerzeel, W. W., van Beek, L. P. H., Konz, M., Shrestha, A. B., and Bierkens, M. F. P.: Hydrological response to climate change in a glacierized catchment in the Himalayas, Clim. Change, 110, 721-736, doi: 10.1007/s10584-011-0143-4, 2012.

Immerzeel, W. W., Wanders, N., Lutz, A. F., Shea, J. M., and Bierkens, M. F. P.: Reconciling high-altitude precipitation in the upper Indus basin with glacier mass balances and runoff, Hydrol. Earth Syst. Sci., 19, 4673-4687, doi: 10.5194/hess-19-4673-2015, 2015.

Jaakko, K. P.: Continuous Snow and Rain Data at 500 to 4400 m Altitude near Annapurna, Nepal, 1999–2001, Arct. Antarct. Alp. Res., 36, 244-248, doi: 10.1657/1523-0430(2004)036[0244:CSARDA]2.0.CO;2, 2004.

Javed, T., Li, Y., Rashid, S., Li, F., Hu, Q., Feng, H., Chen, X., Ahmad, S., Liu, F., and Pulatov, B.: Performance and relationship of four different agricultural drought indices for drought monitoring in China's mainland using remote sensing data, Sci. Total Environ., 759, 143530, doi: 10.1016/j.scitotenv.2020.143530, 2021.

Jie, H. E., and Kun, Y.: China meteorological forcing dataset (1979-2015), National Tibetan Plateau Data Center, doi: 10.3972/westdc.002.2014.db, 2016.

Jin, X., Zhang, L., Gu, J., Zhao, C., Tian, J., and He, C.: Modelling the impacts of spatial heterogeneity in soil hydraulic properties on hydrological process in the upper reach of the Heihe River in the Qilian Mountains, Northwest China, Hydrological Processes, 29, 3318-3327, doi: 10.1002/hyp.10437, 2015.

Kääb, A., Berthier, E., Nuth, C., Gardelle, J., and Arnaud, Y.: Contrasting patterns of early twenty-first-century glacier mass change in the Himalayas, Nature, 488, 495-498, doi: 10.1038/nature11324, 2012.

Kaser, G., Großhauser, M., and Marzeion, B.: Contribution potential of glaciers to water availability in different climate regimes, P. Natl. Acad. Sci. USA, 107, 20223, doi: 10.1073/pnas.1008162107, 2010.

Kayastha, R. B., Steiner, N., Kayastha, R., Mishra, S. K., and McDonald, K.: Comparative Study of Hydrology and Icemelt in Three Nepal River Basins Using the Glacio-Hydrological Degree-Day Model (GDM) and Observations From the Advanced Scatterometer (ASCAT), Front. Earth Sci., doi: 10.3389/feart.2019.00354, 7, 354, 2020.

Keller, R., Clivaz, M., Reynard, E., and Backhaus, N.: Increasing Landscape Appreciation through the Landscape Services Approach. A Case Study from Switzerland, Sustainability, 11, doi: 10.3390/su11205826, 2019.

Kendall, M. G. :Rank correlation methods, Charles Griffin, London, 1975.

Kou, Y. G., and Su, Z.: Variation of precipitation with altitude and its impact on recharge of glaciers in Tuomuer, Chinese Sci. Bull. (in Chinese), 02, 113-115, doi: 10.1360/csb1981-02-113-115, 1981.

Kraaijenbrink, P. D. A., Bierkens, M. F. P., Lutz, A. F., and Immerzeel, W. W.: Impact of a global temperature rise of 1.5 degrees Celsius on Asia's glaciers, Nature, 549, 257-260, doi: 10.1038/nature23878, 2017.

Kumar, N., Ramanathan, A., Arora, A., Soheb, M., Mandal, A., Sharma, P., and Ranjan, S.: Study of isotopic seasonality to assess the water source of proglacial stream in Chhota Shigri Glaciated Basin, Western Himalaya, Hydrol. Process , 34, 1285-1300, doi: 10.1002/hyp.13676, 2020.

Laghari, A. N., Vanham, D., and Rauch, W.: The Indus basin in the framework of current and future water resources management, Hydrol. Earth Syst. Sci., 16, 1063-1083, doi: 10.5194/hess-16-1063-2012, 2012.

Li, H. Y., Zhao, Q. D., Wu, J. H., Ding, Y. J., Qin, J., Wei, H., and Zeng, D.: Quantitative simulation of the runoff components and its variation characteristics in the upstream of the Shule River, J. Glaciol. Geocryol. (in Chinese), 41(4), 907-917, doi: 10.7522/j.issn.1000-0240.2019.0115, 2019.

Li, L. H., Shang, M., Zhang, M. S., Ahmad, S., and Huang, Y.: Snowmelt runoff simulation driven by APHRODITE precipitation dataset. Advances in Water Science (in Chinese), 25, 53-59, doi: 10.14042/j.cnki.32.13.9.2014.01.008, 2014.

Li, Q., Chen, Y., Shen, Y., Li, X., and Xu, J.: Spatial and temporal trends of climate change in Xinjiang, China, J. Geogr. Sci. 21, 1007, doi: 10.1007/s11442-011-0896-8, 2011.

Li, X., Cheng, G., Ge, Y., Li, H., Han, F., Hu, X., Tian, W., Tian, Y., Pan, X., Nian, Y., Zhang, Y., Ran, Y., Zheng, Y., Gao, B., Yang, D., Zheng, C., Wang, X., Liu, S., and Cai, X.: Hydrological Cycle in the Heihe River Basin and Its Implication for Water Resource Management in Endorheic Basins, J. Geophys. Res. Atmos., 123, 890-914, doi: 10.1002/2017JD027889, 2018.

Lin, H. X., Huang, J. C., Xiao, C. D., Qi, X. X., and Chen, Y. N.: Theories and methods on comprehensive regionalization of cryospheric services. Acta Geographica Sinica (in Chinese), 75, 631-646, doi: 10.11821/dlxb202003014, 2020.

Liu, J., Long, A. H., Li, J., Yu, W. J., and Zhang, J.: Analysis on runoff evolution laws and trends of three source-streams of Tarim River in recent 60 years. Water Resources and Hydropower Engineering (in Chinese), 50, 10-17, doi: 10.13928/j.cnki.wrahe.2019.12.002, 2019.

Liu, S. Y., Yao, X. J., Guo, W. Q., Xu, J. L., Shangguan, D. H., Wei, J. F., Bao, W. J., and Wu, L. Z., (2015): The contemporary glaciers in China based on the Second Chinese Glacier Inventory, Acta Geographica Sinica (in Chinese), 70, 3-16, doi: 10.11821/dlxb201501001, 2015.

Liu, Y., Zhang, P., Nie, L., Xu, J., Lu, X., and Li, S.: Exploration of the Snow Ablation Process in the Semiarid Region in China by Combining Site-Based Measurements and the Utah Energy Balance Model—A Case Study of the Manas River Basin, Water, 11, doi: 10.3390/w11051058, 2019.

López-Granados, F., Jurado-Expósito, M., Peña-Barragán, J. M., and García-Torres, L.: Using geostatistical and remote sensing approaches for mapping soil properties, Eur. J. Agron., 23, 279-289, doi: 10.1016/j.eja.2004.12.003, 2005.

Mann, H. B.: Nonparametric Tests Against Trend, Econometrica, 13, 245-259, doi: 10.2307/1907187, 1945.

Mardan, A., Mamattursun, E., Hamit, Y., Gulziba, A., and Yasinjan, M.: Runoff Variation Characteristics in Ebinur Lake Basin During 1964-2012. Chinese Agricultural Science Bulletin (in Chinese), 32, 67-73, doi: 10.11924/j.issn.1000-6850.casb15110147, 2016.

Martín-López, B., Leister, I., Lorenzo Cruz, P., Palomo, I., Grêt-Regamey, A., Harrison, P. A., Lavorel, S., Locatelli, B., Luque, S., and Walz, A.: Nature's contributions to people in mountains: A review, PLoS ONE, 14, e0217847, doi: 10.1371/journal.pone.0217847, 2019.

Mimeau, L., Esteves, M., Zin, I., Jacobi, H. W., Brun, F., Wagnon, P., Koirala, D., and Arnaud, Y.: Quantification of different flow components in a high-altitude glacierized catchment (Dudh Koshi, Himalaya): some cryospheric-related issues, Hydrol. Earth Syst. Sci., 23, 3969-3996, doi: 10.5194/hess-23-3969-2019, 2019.

Mishra, S. K., Jain, S., Salunke, P., and Sahany, S.: Past and future climate change over the Himalaya–Tibetan Highland: inferences from APHRODITE and NEX-GDDP data, Clim. Change, 156, 315-322, doi: 10.1007/s10584-019-02473-y, 2019.

Noël, B., Jakobs, C. L., van Pelt, W. J. J., Lhermitte, S., Wouters, B., Kohler, J., Hagen, J. O., Luks, B., Reijmer, C. H., van de Berg, W. J., and van den Broeke, M. R.: Low elevation of Svalbard glaciers drives high mass loss variability, Nat. Commun., 11, 4597, doi: 10.1038/s41467-020-18356-1, 2020.

Piao, S., Ciais, P., Huang, Y., Shen, Z., Peng, S., Li, J., Zhou, L., Liu, H., Ma, Y., Ding, Y., Friedlingstein, P., Liu, C., Tan, K., Yu, Y., Zhang, T., and Fang, J.: The impacts of climate change on water resources and agriculture in China, Nature, 467, 43-51, doi: 10.1038/nature09364, 2010.

Pritchard, H. D.: Asia's shrinking glaciers protect large populations from drought stress, Nature, 569, 649-654, doi: 10.1038/s41586-019-1240-1, 2019.

Qin, D., Zhou, B., and Xiao, C.: Progress in studies of cryospheric changes and their impacts on climate of China, J. Meteorol. Res., 28, 732-746, doi: 10.1007/s13351-014-4029-z, 2014.

Rasul, G. and Molden, D.: The Global Social and Economic Consequences of Mountain Cryospheric Change, Front. Environ. Sci., 7, 91, doi: 10.3389/fenvs.2019.00091, 2019.

Rasul, G., Pasakhala, B., Mishra, A., and Pant, S.: Adaptation to mountain cryosphere change: issues and challenges, Climate and Development, 12, 297-309, doi: 10.1080/17565529.2019.1617099, 2020.

RGI Consortium, Randolph Glacier Inventory – A Dataset of Global Glacier Outlines: Version 6.0: Technical Report, Global Land Ice Measurements from Space, Colorado, USA, Digital Media, doi: 10.7265/N5-RGI-60, 2017.

Rounce, D. R., Hock, R., and Shean, D. E.: Glacier Mass Change in High Mountain Asia Through 2100 Using the Open-Source Python Glacier Evolution Model (PyGEM), Front. Earth Sci., 7, 331, doi: 10.3389/feart.2019.00331, 2020a.

Rounce, D. R., Khurana, T., Short, M. B., Hock, R., Shean, D. E., and Brinkerhoff, D. J.: Quantifying parameter uncertainty in a large-scale glacier evolution model using Bayesian inference: application to High Mountain Asia, J. Glaciol. , 66, 175-187, doi: 10.1017/jog.2019.91, 2020b.

Sakai, A.: GAMDAM glacier inventory for High Mountain Asia, doi: 10.1594/PANGAEA.891423, 2018.

Sakai, A., Nuimura, T., Fujita, K., Takenaka, S., Nagai, H., and Lamsal, D.: Climate regime of Asian glaciers revealed by GAMDAM glacier inventory, Cryosphere, 9, 865-880, doi: 10.5194/tc-9-865-2015, 2015.

Shean, D. E., Bhushan, S., Montesano, P., Rounce, D. R., Arendt, A., and Osmanoglu, B.: A Systematic, Regional Assessment of High Mountain Asia Glacier Mass Balance, Front. Earth Sci., 7, 363, doi: 10.3389/feart.2019.00363, 2020.

Shen, Y. P., and Liang, H.: High recipitation in Glacial Region of High Mountains in High Asia: Possible Cause. J. Glaciol. Geocryol. (in Chinese), 26, 806-809, doi: 10.7522/j.issn.1000-0240.2004.06.0806.04, 2004.

Shi, Y., Liu, G., Zhang, B., & Meng, X. (2003). Concept design of dynamic regulation system of oasis ecosystem (Vol. 4890): SPIE.

https://doi.org/10.5194/hess-2021-377
Preprint. Discussion started: 22 September 2021

Sorg, A., Bolch, T., Stoffel, M., Solomina, O., and Beniston, M.: Climate change impacts on glaciers and runoff in Tien Shan (Central Asia), Nature Climate Change, 2, 725-731, doi: 10.1038/nclimate1592, 2012.

Srivastava, P., Bhambri, R., Kawishwar, P., and Dobhal, D. P.: Water level changes of high altitude lakes in Himalaya–Karakoram from ICESat altimetry, Journal of Earth System Science, 122, 1533-1543, doi: 10.1007/s12040-013-0364-1, 2013.

Su, X. M., Liu, Z. H., Wei, T. F., Wang, Y. J., and Liu, Y.: Change of Ebinur Lake Area and Its Respose Characteristics of the Runoff Change. Research of Soil and Water Conservation (in Chinese), 23(3), 252-256, doi: 10.13869/j.cnki.rswc.2016.03.043, 2016.

Sun, M., Liu, S., Yao, X., Guo, W., and Xu, J.: Glacier changes in the Qilian Mountains in the past half-century: Based on the revised First and Second Chinese Glacier Inventory, Journal of Geographical Sciences, 28, 206-220, doi: 10.1007/s11442-018-1468-y, 2018.

Sun, M., Ma, W., Yao, X., Zhao, L., Li, Z., and Qin, D.: Evaluation and spatiotemporal characteristics of glacier service value in the Qilian Mountains, J. Geogr. Sci., 30, 1233-1248, doi: 10.1007/s11442-020-1779-7, 2020.

Tak, S. and Keshari, A. K.: Investigating mass balance of Parvati glacier in Himalaya using satellite imagery based model, Sci. Rep., 10, 12211, doi: 10.1038/s41598-020-69203-8, 2020.

Tan, X., Ma, Z., He, K., Han, X., Ji, Q., and He, Y.: Evaluations on gridded precipitation products spanning more than half a century over the Tibetan Plateau and its surroundings, J. Hydrol., 582, 124455, doi: 10.1016/j.jhydrol.2019.124455, 2020.

Tang, M. C.: The distribution of precipitation in Mountain Qilian (Nanshan), Acta Geographica Sinica (in Chinese), 40, 323-332, doi: 10.11821/dlxb198504017, 1985.

Tang, J., Yang, Y., Xiong, Z., and Dong, X.: Evaluation of High-Resolution Gridded Precipitation Data in Arid and Semiarid Regions: Heihe River Basin, Northwest China, Journal of Hydrometeorology, 18, 3075-3101, doi: 10.1175/JHM-D-16-0252.1, 2017.

Thomas, A.: The Climate of the Gongga Shan Range, Sichuan Province, PR China, Arct. Alp. Res., 29, 226-232, doi: 10.1080/00040851.1997.12003237, 1997.

Waldron, B., Gui, D., Liu, Y., Feng, L., and Dai, H.: Assessing water distribution and agricultural expansion in the Cele Oasis, China, Environ. Monit. Assess., 192, 288, doi: 10.1007/s10661-020-8233-2, 2020.

Wang, P., Li, Z., Zhou, P., Wang, W., Jin, S., Li, H., Wang, F., Yao, H., Zhang, H., and Wang, L.: Recent changes of two selected glaciers in Hami Prefecture of eastern Xinjiang and their impact on water resources, Quatern. Int., 358, 146-152, doi: 10.1016/j.quaint.2014.05.028, 2015.

Wang, R., Liu, S., Shangguan, D., Radić, V., and Zhang, Y.: Spatial Heterogeneity in Glacier Mass-Balance Sensitivity across High Mountain Asia, Water, 11, doi: 10.3390/w11040776, 2019.

https://doi.org/10.5194/hess-2021-377
Preprint. Discussion started: 22 September 2021

Wang, S. J., Zhou, L. Y., Dou, W. K., Jie, J., and Ma, X. K.: Evaluation of Glacier Tourism Service Potential in Different Periods based on GIS-Taking Xinjiang Uygur Autonomous Region as an Example. Remote Sensing Technology and Application (in Chinese), 35, 1283-1291, doi: 10.11873/j.issn.1004-0323.2020.6.1283, 2020.

Wang, T., Zhao, Y., Xu, C., Ciais, P., Liu, D., Yang, H., Piao, S., and Yao, T.: Atmospheric dynamic constraints on Tibetan Plateau freshwater under Paris climate targets, Nature Climate Change, 11, 219-225, doi: 10.1038/s41558-020-00974-8, 2021.

Wang, W., Sun, L., Cai, Y., Yi, Y., Yang, W., and Yang, Z.: Evaluation of multi-source precipitation data in a watershed with complex topography based on distributed hydrological modeling, River Res. Appl., doi: 10.1002/rra.3681, 2020.

Wang, X. J: Hydrological response to atmospheric temperature changes in the Qaidam Basin and its surroundings over past 60 years. (Master's thesis). Retrieved from Cnki. (https://kns.cnki.net/KCMS/detail/detail.aspx?dbname=CMFD202001&filename=1019674546.nh). Xi'an, CHN: Chang'an University, 2019.

Warren, F. J., and Lemmen, D. S.: Canada in a changing climate: Sector perspectives on impacts and adaptation: Government of Canada. https://www.nrcan.gc.ca/sites/www.nrcan.gc.ca/files/earthsciences/pdf/assess/2014/pdf/Full-Report_Eng.pdf, 2014.

Wortmann, M., Bolch, T., Menz, C., Tong, J., and Krysanova, V.: Comparison and Correction of High-Mountain Precipitation Data Based on Glacio-Hydrological Modeling in the Tarim River Headwaters (High Asia), Journal of Hydrometeorology, 19, 777-801, doi: 10.1175/JHM-D-17-0106.1, 2018.

Wu, J., Guo, S., Huang, H., Liu, W., and Xiang, Y.: Information and Communications Technologies for Sustainable Development Goals: State-of-the-Art, Needs and Perspectives, IEEE Communications Surveys & Tutorials, 20, 2389-2406, doi: 10.1109/COMST.2018.2812301, 2018.

Xu, B., Lu, Z., Liu, S., Li, J., Xie, J., Long, A., Yin, Z., and Zou, S.: Glacier changes and their impacts on the discharge in the past half-century in Tekes watershed, Central Asia, Physics and Chemistry of the Earth, Parts A/B/C, 89-90, 96-103, doi: 10.1016/j.pce.2015.03.003, 2015.

Yang, C., Lan, Y., Wang, N., Wang, Q., and Li, Y.: Mountainous runoff changes and climate factors analysis of the Shule River Basin in 1958-2015. Scientia Geographica Sinica (in Chinese), 37, 1894, doi: 10.13249/j.cnki.sgs.2017.12.013, 2017.

Yang, J. P., Ding, Y. J., and Fang, Y. P.: Adaptation research of cryosphere change in China: advances and prospections. Climate Change Research (in Chinese), 15, 178-186, doi: 10.12006/j.issn.1673-1719.2018.080, 2019.

Yang, Y., Wang, G., Wang, L., Yu, J., and Xu, Z.: Evaluation of Gridded Precipitation Data for Driving SWAT Model in Area Upstream of Three Gorges Reservoir, PLoS ONE, 9, e112725, doi: 10.1371/journal.pone.0112725, 2014.

Yang, Y., Wu, Q., and Jin, H.: Evolutions of water stable isotopes and the contributions of cryosphere to the alpine river on the Tibetan Plateau, Environmental Earth Sciences, 75, 49, doi: 10.1007/s12665-015-4894-5, 2015.

Yao, T., Li, Z., Yang, W., Guo, X., Zhu, L., Kang, S., Wu, Y., and Yu, W.: Glacial distribution and mass balance in the Yarlung Zangbo River and its influence on lakes, Chin. Sci. Bull., 55, 2072-2078, doi: 10.1007/s11434-010-3213-5, 2010.

Yatagai, A., Krishnamurti, T. N., Kumar, V., Mishra, A. K., and Simon, A.: Use of APHRODITE Rain Gauge?Based Precipitation and TRMM 3B43 Products for Improving Asian Monsoon Seasonal Precipitation Forecasts by the Superensemble Method, J. Clim., 27, 1062-1069, doi: 10.1175/JCLI-D-13-00332.1, 2014.

Ye, Z., Liu, H., Chen, Y., Shu, S., Wu, Q., and Wang, S.: Analysis of water level variation of lakes and reservoirs in Xinjiang, China using ICESat laser altimetry data (2003–2009), PLoS ONE, 12, e0183800, doi: 10.1371/journal.pone.0183800, 2017.

Zarfl, C., Lumsdon, A. E., Berlekamp, J., Tydecks, L., and Tockner, K.: A global boom in hydropower dam construction, Aquat. Sci., 77, 161-170, doi: 10.1007/s00027-014-0377-0, 2015.

Zhang, A., Liu, W., Yin, Z., Fu, G., and Zheng, C.: How Will Climate Change Affect the Water Availability in the Heihe River Basin, Northwest China?, J. Hydrometeorol., 17, 1517-1542, doi: 10.1175/JHM-D-15-0058.1, 2016a.

Zhang, G.: The Study of Glacier Changes in the Gongga Mountains. (Doctoral dissertation). Retrieved from Cnki. (https://kns.cnki.net/KCMS/detail/detail.aspx?dbname=CDFD1214&filename=1013122660.nh). Lanzhou, CHN: Lanzhou University, 2012.

Zhang, G., Xie, H., Yao, T., Li, H., and Duan, S.: Quantitative water resources assessment of Qinghai Lake basin using Snowmelt Runoff Model (SRM), J. Hydrol., 519, 976-987, doi: 10.1016/j.jhydrol.2014.08.022, 2014.

Zhang, H. Y.: Precipitation Gradient in Tianshan Mountain Area Based on Multi-Source Precipitation Data. (Master's thesis). Retrieved from Cnki. (https://kns.cnki.net/KCMS/detail/detail.aspx?dbname=CMFD202101&filename=1020977265.nh). Lanzhou, CHN: Northwest Normal University, 2020.

Zhang, Q., Yang, J., Wang, W., Ma, P., Lu, G., Liu, X., Yu, H., and Fang, F.: Climatic Warming and Humidification in the Arid Region of Northwest China: Multi-Scale Characteristics and Impacts on Ecological Vegetation, J. Meteorol. Res., 35, 113-127, doi: 10.1007/s13351-021-0105-3, 2021.

Zhang, S. Q., Gao, X., and Zhang, X. W.: Glacial runoff likely reached peak in the mountainous areas of the Shiyang River Basin, China, J. Mt. Sci., 12, 382-395, doi: 10.1007/s11629-014-3077-2, 2015.

Zhang, S., Gao, X., Ye, B., Zhang, X., and Hagemann, S.: A modified monthly degree-day model for evaluating glacier runoff changes in China. Part II: application, Hydrol. Process, 26, 1697-1706, doi: 10.1002/hyp.8291, 2012.

Zhang, Y., Liu, S., and Ding, Y.: Observed degree-day factors and their spatial variation on glaciers in western China, Ann. Glaciol., 43, 301-306, doi: 10.3189/172756406781811952, 2006.

Zhang, Y., Tuerxunbai, G., Su, L., and Qianqian, L.: Spatial and temporal characteristics of climate change at different altitudes in Xinjiang in the past 60 years, Arid Land Geography (in Chinese), 42, 822-829: doi: 10.12118/j.issn.1000-6060.2019.04.13, 2019.

Zhang, Y., Luo, Y., Sun, L., Liu, S., Chen, X., and Wang, X.: Using glacier area ratio to quantify effects of melt water on runoff, J. Hydrol., 538, 269-277, doi: 0.1016/j.jhydrol.2016.04.026, 2016b.

Zhang, Z., Liu, L., He, X., Li, Z., and Wang, P.: Evaluation on glaciers ecological services value in the Tianshan Mountains, Northwest China, J. Geogr. Sci., 29, 101-114, doi: 10.1007/s11442-019-1586-1, 2019.

Zhao, C. Y., Shi, F. Z., Sheng, Y., Li, J., Zhao, Z. M., Han, M., and Yilihamu, Y.: Regional Differentiation Characteristics of Precipitation Changing with Altitude in Xinjiang Region in Recent 50 Years. J. Glaciol. Geocryol. (in Chinese), 33, 1203-1213, doi: 10.7522/j.issn.1000-0240.2011.06.1203.11, 2011.

Zhu, G., Guo, H., Qin, D., Pan, H., Zhang, Y., Jia, W., and Ma, X.: Contribution of recycled moisture to precipitation in the monsoon marginal zone: Estimate based on stable isotope data, J. Hydrol., 569, 423-435, doi: 10.1016/j.jhydrol.2018.12.014, 2019.

Table

Table 1

Annual precipitation and area of OAA in each watershed

Watershed	Annual precipitation (mm)	Area of OAA (km^2)
Pai Basin	93.06	1047.50
Shule River Basin	79.10	2913.70
Hami Basin	63.53	1585.64
Turpan Basin	75.94	2218.58
Kai-kong River Basin	103.92	10191.39
Hotan River Basin	39.04	4816.73
Western Qaidam Basin	~ 0	538.37
Eastern Qaidam Basin	~ 0	876.23
Kriya Rivers Basin	51.31	2308.90
Qarqan Rivers Basin	78.82	1362.69
Easter Rivers Basin	139.52	5487.35
Middle Rivers Basin	175.29	21699.18
Yarkand River Basin	99.87	13568.21
Kashgar River Basin	137.61	11027.69
Weigan River Basin	136.96	8632.32
Aksu River Basin	148.64	10276.95
Qinghai Lake Drainage System	323.09	1012.96

https://doi.org/10.5194/hess-2021-377
Preprint. Discussion started: 22 September 2021

Hydrology and Earth System Sciences Discussions

Ebinur Lake Drainage System	191.29	11366.95
Heihe River Basin	113.67	9273.28
Shiyang River Basin	198.63	9333.13
Ili River Basin	299.05	13332.06
Datong River Above Hall	410.38	1069.43

Table 2

H_{map} and H_{max} used in this paper. *H_{map} in Eastern Kunlun and Western Kunlun were speculated by five other regions that had references about maximum rainfall height. H_{max} refers to the average of the maximum height of each glacier in regions of RGI 6.0.*

Region	H_{map}	H_{max}
Qilian Shan	4200 (Chen et al., 2018; Wang et al., 2009)	5500
Eastern Tien Shan	3000 (Zhang, Tuerxunbai, et al., 2019)	5000
Western Tien Shan	3000 (Zhang, Tuerxunbai, et al., 2019)	6000
Eastern Kunlun	4500	6500
Western Kunlun	4000	6500
Karakoram	2500 (Immerzeel et al., 2012)	7500
Pamir	3000 (Hewitt, 2007)	6500

Figure

Figure 1

https://doi.org/10.5194/hess-2021-377
Preprint. Discussion started: 22 September 2021

Locations of watersheds and oasis agriculture areas affected by glaciers in the dryland areas of China.

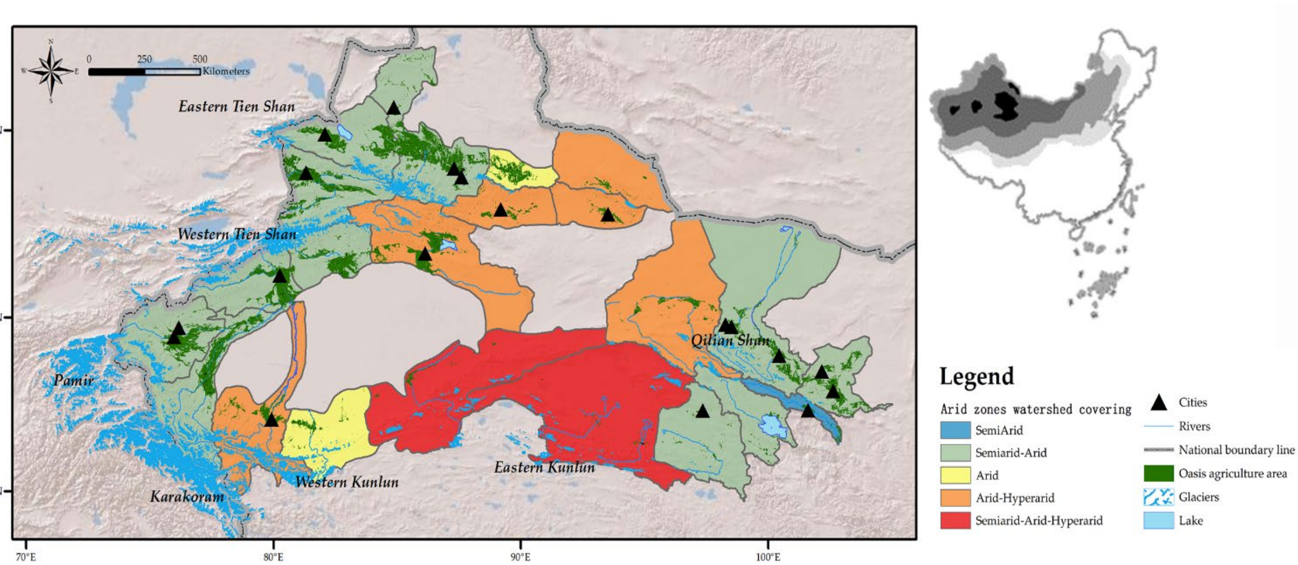

Note. (Shades of color indicate drought from subhumid – semiarid – arid – hyper-arid) and the tertiary watersheds in the dryland areas of China affected by the Qilian Shan, Western Tien Shan, Eastern Tien Shan, Western Kunlun, Eastern Kunlun, Karakoram and Pamir. Oasis agricultural areas exist along rivers that originate from glaciers, and cities are built around oases. World Shaded Relief provided by Esri (http://goto.arcgisonline.com/maps/World_Shaded_Relief) and the Chinese map was from Resource and Environment Science and Data Centre, Chinese Academy of Sciences (https://www.resdc.cn/data.aspx?DATAID=205)

Figure 2

Map of total glacier runoff.

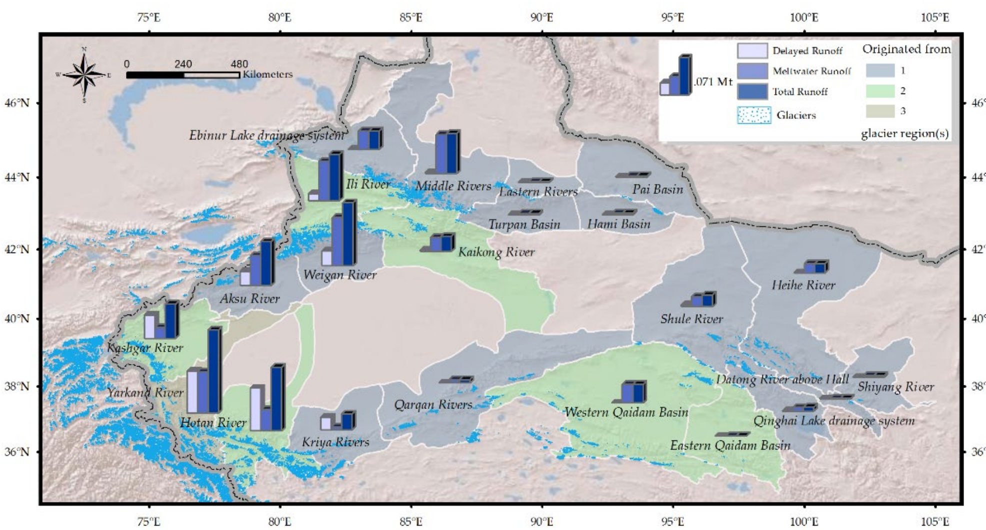

Note. Distribution of total glacier runoff, including delayed runoff and meltwater runoff. Shown are the average amount of runoff for every study basin in the DAC for the period 1961-2015.

Figure 2

Map of total glacier runoff.

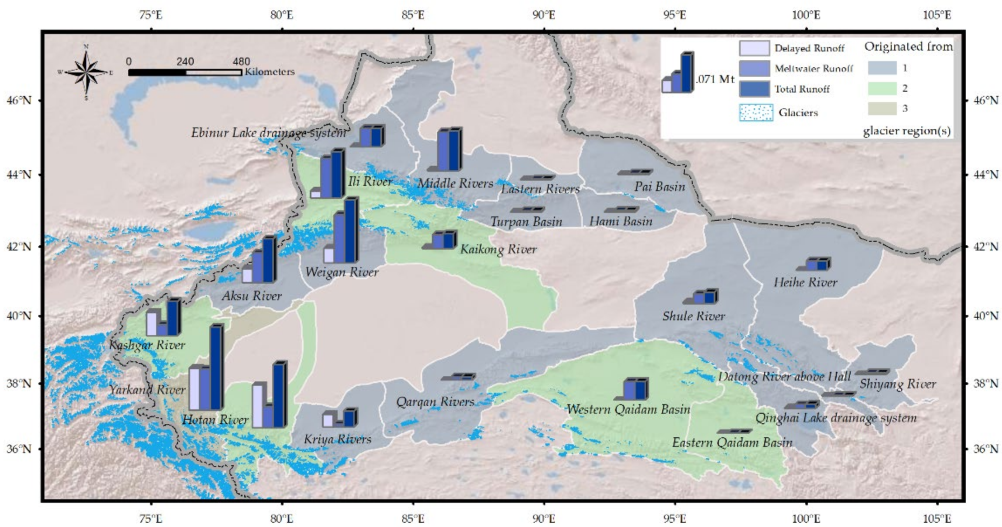

Note. Distribution of total glacier runoff, including delayed runoff and meltwater runoff. Shown are the average amount of runoff for every study basin in the DAC for the period 1961-2015. World Shaded Relief provided by Esri (http://goto.arcgisonline.com/maps/World_Shaded_Relief).

Hydrology and Earth System Sciences
Discussions

974 **Figure 3**

975 Map of glacier runoff validation.

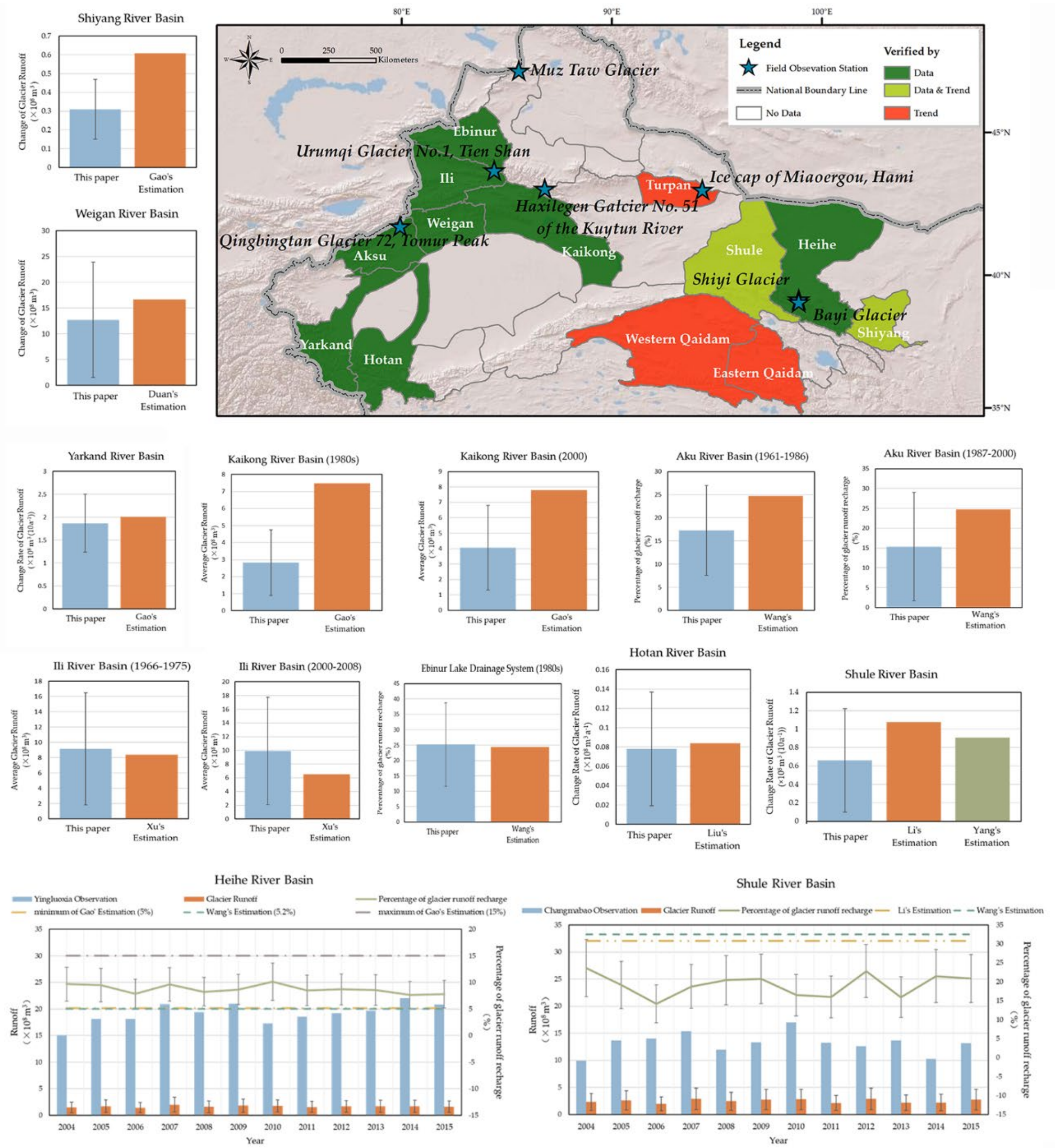

976 *Note.* Some basins had relevant data verification, some basins had both data and trend verification, some basins had only
977 trend verification, and the areas without color lacked data. The study on glacier runoff in the DAC was unevenly
978 distributed. The blue color in each chart was the glacier runoff calculated in this paper, and the other colors represented
979 runoff obtained in different studies. World Shaded Relief provided by Esri
980 (http://goto.arcgisonline.com/maps/World_Shaded_Relief).

Figure 4

Statistical maps of different types and quantities of glaciers in each basin.

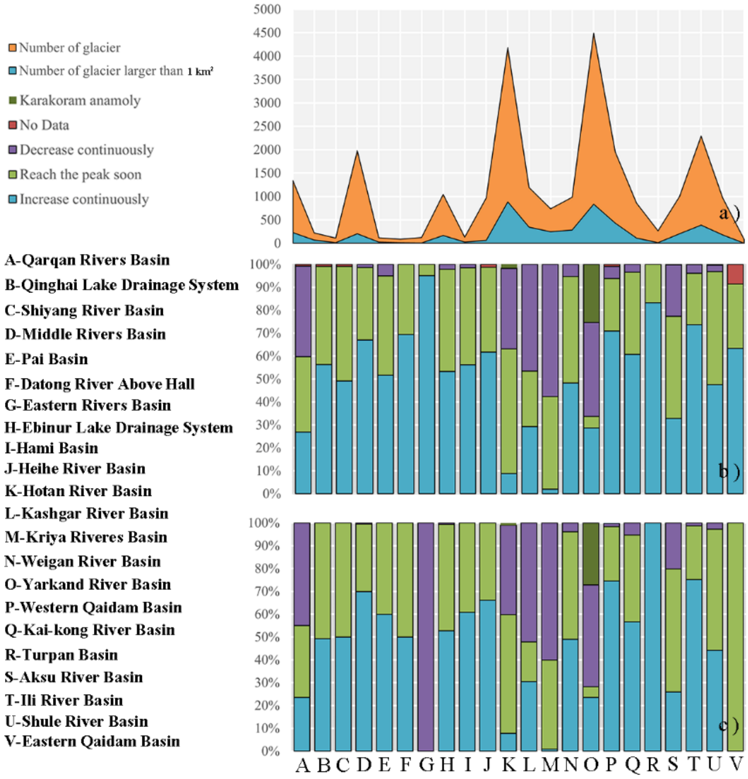

Note. a) Stacked area chart of the number of glaciers and glaciers larger than 1 km^2. b) Stacked bar chart of different types of glaciers under future changes. c) Stacked bar chart of different types of glaciers larger than 1 km^2 under future changes.

https://doi.org/10.5194/hess-2021-377
Preprint. Discussion started: 22 September 2021

Figure 5

Mann-Kendall Test of total glacier runoff with a confidence of 95%.

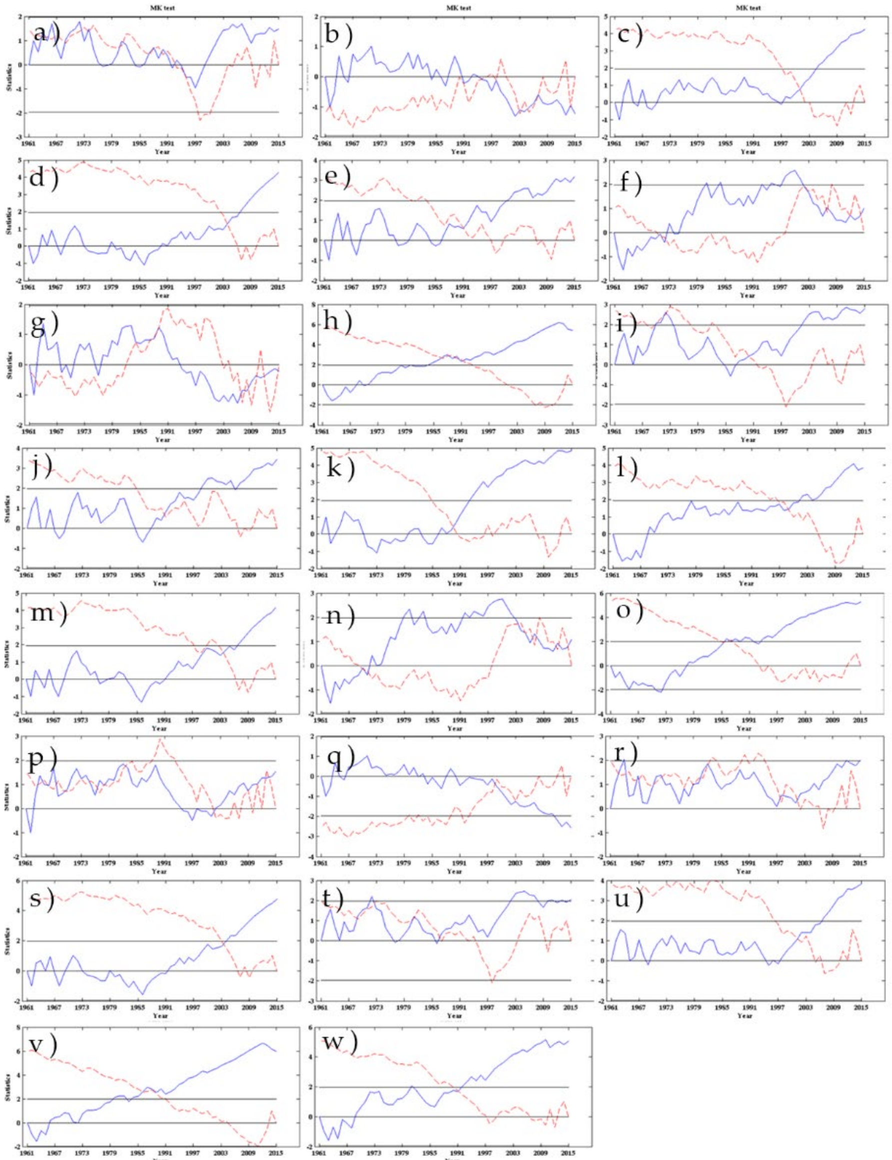

Note. in a)Aksu River Basin, b)Datong River Above Hall, c)Eastern Qaidam Basin, d)Eastern Rivers Basin, e)Ebinur Lake Drainage System, f)Hami Basin, g)Heihe River Basin, h)Hotan River Basin, i)Ili River Basin, j)Kai-kong River Basin, k)Kashgar River Basin, l)Kriya Rivers Basin, m)Middle Rivers Basin, n)Pai Basin, o)Qarqan Rivers Basin, p)Qinghai Lake Drainage System, q)Shiyang River Basin, r)Shule River Basin, s)Turpan Basin, t)Weigan River Basin, u)Western Qaidam Basin, v)Yarkand River Basin, w)Entire Basins. **Blue line referred to the UF curve and red line referred to the UB curve.**

https://doi.org/10.5194/hess-2021-377
Preprint. Discussion started: 22 September 2021

Figure 6

Spatiotemporal regime of glacier runoff in the DAC. a) the trend of glacier runoff, b) the year with a significant trend, and c) the average rate of glacier runoff change.

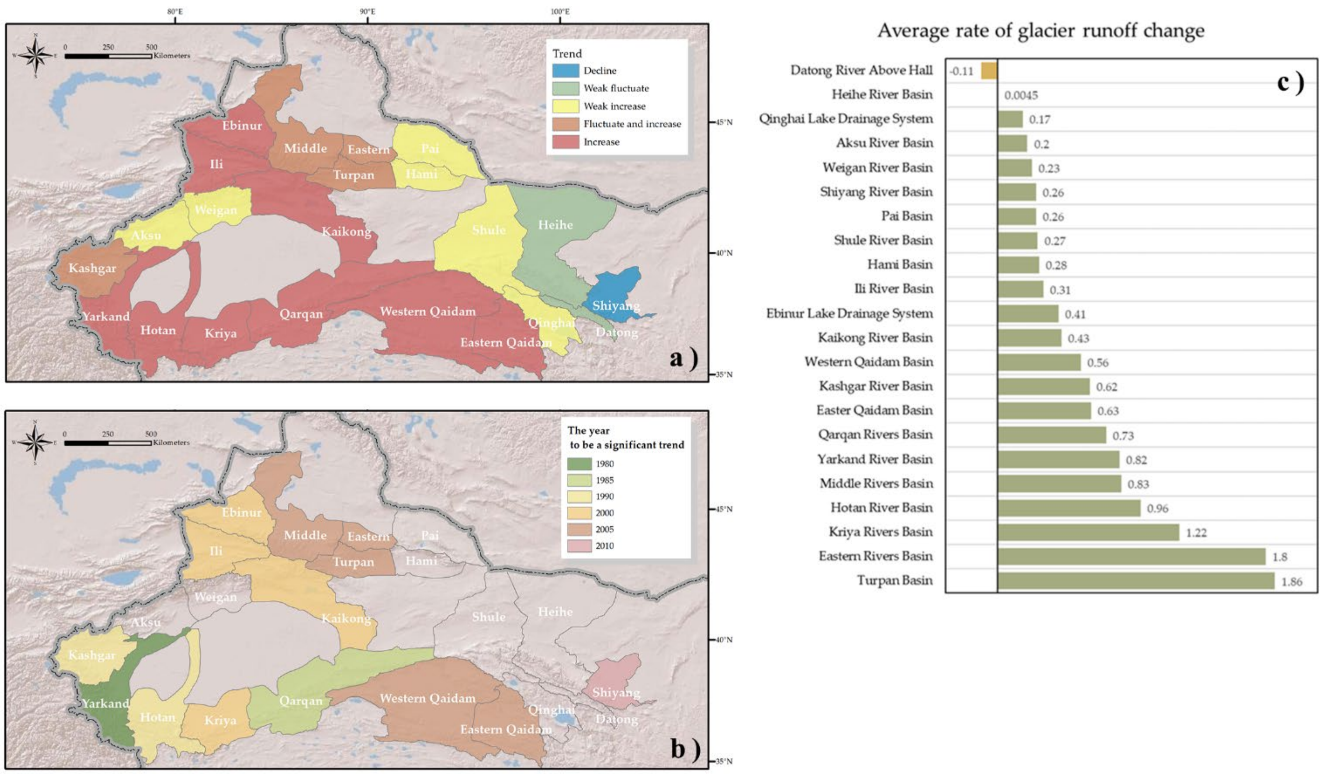

Note. The trends classified as "weak fluctuating" and "weak increase" had no significant time. Except for Shiyang River basin and Datong River above Hall, glacier runoff increased from 1961 to 2015. World Shaded Relief provided by Esri (http://goto.arcgisonline.com/maps/World_Shaded_Relief).

https://doi.org/10.5194/hess-2021-377
Preprint. Discussion started: 22 September 2021

Hydrology and Earth System Sciences
Open Access
EGU
Discussions

Figure 7

Box plots of precipitation gradients for $\Delta H + (H_{max} - H)$ (m) and each glacier region.

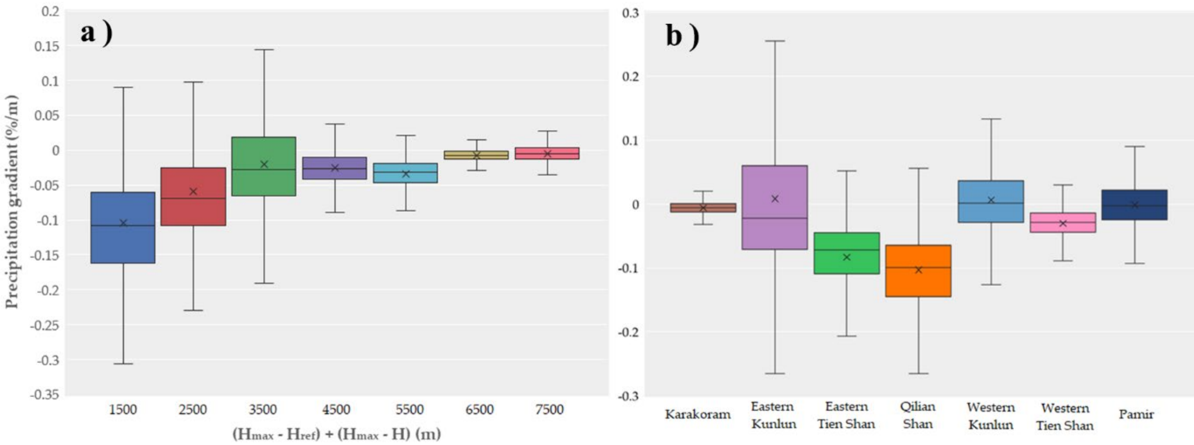

Note. Line: median; multiple sign: average number; box: 25–75% of the observations; whiskers: min and max non-outliers.

Figure 8

Proportion of delayed runoff and meltwater runoff to a) agricultural water consumption, b) municipal water consumption and c) industrial water consumption.